ABSTRACT

R.M. Pratt: A Vehicular Portal Monitor

A NaI monitoring system was assembled and installed to provide radiological surveillance of refuse trucks destined for the sanitary landfill at Brookhaven National Laboratory. The performance of the system was tested by obtaining count rates for various gamma reference sources placed in the bed of a pickup truck parked over the detector. The system's sensitivity was documented for the various sources counted in a stationary truck as well as in a truck moving over the detector. Data analysis also determined the lower limits of detection for the system.

Performance testing of the vehicular portal monitor suggest that it can detect μCi amounts of radionuclides on a truck.

ACKNOWLEDGEMENTS

Those to whom I am indebted are many. First and foremost, I offer my gratitude to Dr. James Watson for his extraordinary abilities as an educator. His support and guidance made possible my most valuable learning experience.

I also express my appreciation to Dr. Joseph Shonka of Brookhaven National Laboratory without whose knowledge, strength and advice this project would not have taken root. I would like to thank the staff of Brookhaven's Safety and Environmental Protection Division, namely Messrs. Joseph Balsamo, Joseph Klemish, George Hughes and Allen Jones for their cheerful assistance.

Finally, my heartfelt thanks go to my parents for their love, patience and endless generosity.

TABLE OF CONTENTS

LIST OF FIGURES

LIST OF TABLES

Chapter I

INTRODUCTION

Objective

The purpose of this project was to design, assemble and test a prototype vehicular monitoring system to detect inadvertent radioactivity on refuse trucks destined for the sanitary landfill at Brookhaven National Laboratory (BNL). Located in Upton, L.I., N.Y., BNL has operated as a research facility devoted to peaceful uses of atomic energy since 1947. Radioactive waste generated at the laboratory is handled on-site at the Hazardous Waste Management Facility. The sanitary landfill at Brookhaven is designated to receive all non-toxic waste generated by the various research facilities.

Routine radiological surveys at BNL have indicated the presence of small quantities of activated or contaminated waste in the landfill. For this reason the Safety and Environmental Protection Division (SEPD) of BNL has committed itself to initiate radiological surveillance of refuse traffic destined for the landfill.

To this end, a vehicular portal monitor (VPM) was assembled and tested. The procedures and results of this undertaking are documented in this report.

Data generated in practical application of the VPM will be collected and analyzed periodically by the SEPD staff. The number of trucks carrying refuse to the landfill and the proportion of contaminated traffic will be determined. These results will be a decision factor for the installation of a permanent vehicular portal monitor at the landfill.

Scope

The scope of the project was to assemble, install and test the prototype VPM using a NaI crystal as a means of detection. The NaI detector head was assembled and buried at a test site at the side of the primary access road leading to the landfill. The associated electronics of the system were installed at the site and protected from environmental conditions by a custom-made wooden housing. The system was powered by a 110 volt power supply. An aluminum plate was placed over the face of the detector head to protect it from the passage of vehicles.

The system was automated to document the passage of a vehicle and record the level of radioactivity detected during a counting interval activated by a pressure tube tripping device. Radiation levels on a truck were determined by recording count rates with a counter/timer and a strip chart recorder. The system was also designed to record background radiation in hourly counts around-the-clock.

Performance testing of the VPM involved the determination of detection sensitivity for various nuclides counted on a stationary truck parked over the detector. Sensitivity for nuclides counted on a truck moving at 5 mph over the detector was also considered in this study. Further analysis of the counting data determined lower limits of detection (LLD) for each nuclide on both a stationary and moving vehicle.

<u>Other Vehicular Portal Monitors</u>

A computer search of nationwide literature performed at the BNL library yielded no information on vehicular portal monitors employing a NaI crystal as a means of detection. One commercially available system designed to monitor vehicles was found. It was manufactured by the IRT Corporation of San Diego, California and operated on the principle of liquid scintillation detection (Ba 84).

The only vehicular portal monitor based on NaI detection was one custom-designed by the Health Physics personnel at Los Alamos National Laboratory (LANL) in New Mexico. This detector had gained some fame by detecting a truckload of contaminated metal which originated at the Jonke Fenix scrap metal yard in Juarez, Mexico. It was this device that triggered an investigation leading to the discovery of the Juarez incident where recycled metal was contaminated with ^{60}Co from a radiotherapy unit that was discarded at the Jonke Fenix scrap metal yard (He 84).

The monitoring system at LANL used a 5 x 2 inch NaI crystal located beneath an aluminum manhold cover in the road at the gate of an accelerator facility. The system made use of two NaI crystals, one above ground and one below ground, to correlate on-vehicle radiation levels with background variability. The LANL system operated on a tripping system which activated the electronics to record data. The system was also designed to photograph any vehicle that triggered a radiation alarm. The written report on the LANL vehicular portal monitor had not been completed and, because of LANL's defense contract, further details concerning this portal monitor were unavailable (Dv 84).

Chapter II

EQUIPMENT AND INSTALLATION

Materials used for fabrication of the VPM and procedures for installation at the test site are discussed in the following sections. All equipment was provided by the Health Physics Instrumentation Shop at BNL. Workbench space was made available in the Calibration Shop for assembly and preliminary testing of the system.

Electronics

A list of the electronic components used in development of the system is given below:

NIM bin

High Voltage Supply, Bertan Model NIM 313

Amp/Preamp, Canberra 814

Amp/TSCA, Canberra Model 2015 A (single channel analyzer)

Counter/Timer, Canberra Model 1776

Serial Scanner/Printer, Canberra Model 2089

LIN/LOG Ratemeter, Canberra Model 1481L

Strip Chart Recorder, Esterline Angus

3 X 3 inch NaI crystal/photomultiplier tube, Harshaw

4 X 2 inch NaI crystal/photomultiplier tube, Harshaw

8 X 8 inch NaI crystal/photomultiplier tube, Harshaw

A schematic of the final assembly of the VPM is given in Figure 1.

Other Equipment

The detector head was assembled in the Calibration Shop. The materials used for fabrication of this unit are listed below:

Baird well-counter lead pig

Large bottomless steel trash container

Insulating foam

Silica gel

Plastic bags

50 foot cables

1 inch thick aluminum plate, 2.5 ft^2.

The Baird well-counter lead pig used in the assembly of the detector head had been designed to meet the specifications of a 3 X 3 inch NaI crystal/photomultiplier tube (PMT). The bottom of the well was fitted with the necessary circuitry for electrical connection of the crystal/PMT unit. Externally, the base of the pig was equipped with connectors for high voltage (HV) and signal cables.

The Baird pig provided several inches of lead around the sides of the NaI crystal to shield it from background radiation and to protect it from environmental conditions at the test site.

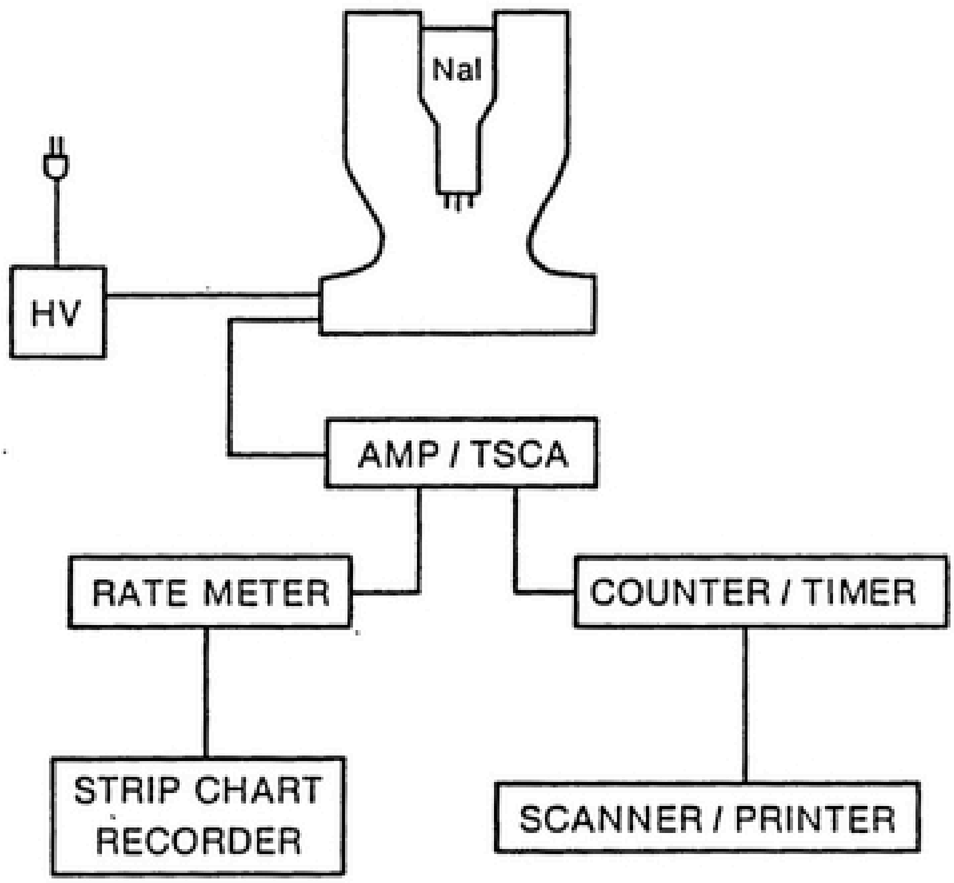

Figure 1. System Schematic

Assembly of Detector Head

To assemble the detector head, the 3 X 3 inch NaI crystal/PMT was permanently encased in the steel trash container in the following manner:

The crystal/PMT unit was fitted into the well of the lead pig to make electrical connection at the base of the well. The HV and signal cables were connected externally at the base of the pig. This entire unit was enveloped in several layers of plastic and silica gel was placed inside the plastic to prevent any moisture from coming into contact with the cable connections.

The pig was then inverted on the floor of the shop and propped up on three bolts to suspend the unit one inch from the floor. The large bottomless trash can was placed on the floor over the pig and centered around it. The power cables, connected at the base of the pig, were positioned along the inside of the can and out over the rim.

The ingredients of an insulating foam were mixed and the solution was poured into the trash can, over and around the lead pig. When it set, the foam rose to surround the pig completely and hardened to fix the detector in place at one end of the steel can. To complete the assembly, the detector face was capped with a thin sheet of aluminum, the edges of which were bent over the sides of the can and taped securely.

This unit comprised the detector head, fully protected from environmental conditions, to be buried at the test site. A diagram of the assembled detector head is given in Figure 2.

Placement of Equipment at Test Site

The test site for the VPM was chosen on the basis of its proximity to the landfill and the availability of a 110 Volt power supply. The site was located next to Building 530 at the corner of Brookhaven Avenue and Seventh Street at the laboratory. The distance between the landfill and the VPM was about a half mile.

The detector head was buried in the ground at the north side of Brookhaven Avenue. The face of the detector was situated in the same plane with the surface of the earth and remained uncovered by soil. A one inch thick, 2.5 ft^2 aluminum plate was placed over the face of the detector to provide protection from the passage of vehicles.

The NIM bin electronics unit was placed adjacent to the 110 Volt outlet which supplied power to it. A custom-made wooden housing, built by the HP Instrumentation staff, protected the electronics from environmental conditions. This unit was supported by four cement blocks and incorporated a vented cupola for cooling by natural convection. The weatherproof housing was fitted with a hinged hatch for access to the front panel controls of the

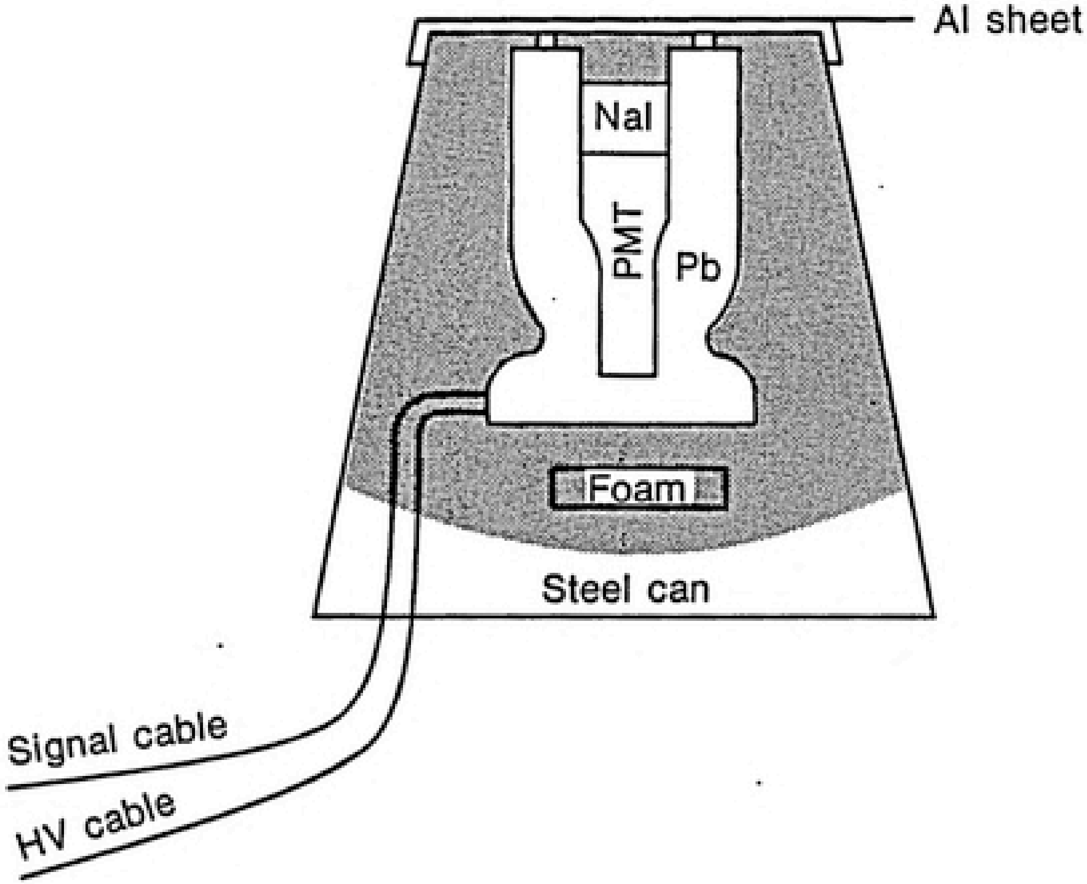

Figure 2. Detector Head Assembly

electronic components. A separate compartment for the strip chart recorder was located on top of the NIM bin compartment under the cupola. Figure 3 gives a diagram of the electronics housing.

The HV and signal cables connecting the detector head to the associated electronics were recessed below ground in a 50 foot trench for protection from lawn mowers.

A pressure tube tripping device, similar to those found at service stations, was fixed above ground about 7 feet in front of the detector head. The pressure tube was connected to the electronics through the underground trench. This device was designed to activate the electronics when tripped by the wheels of a vehicle. Figure 4 gives a diagram of the equipment in place at the VPM test site.

Check Sources

Check sources used for testing the performance of the VPM were gamma reference sources supplied by the Radiochemical Centre, Amersham, England. The kit contained nine point source nuclides encased in rectangular containers measuring 25.4 x 11.0 x 2.0 mm. Each container housed a 1 mm. active bead between 0.5 mm polystyrene windows. The Amersham nuclides, and the activity of each, used in this project are listed below.

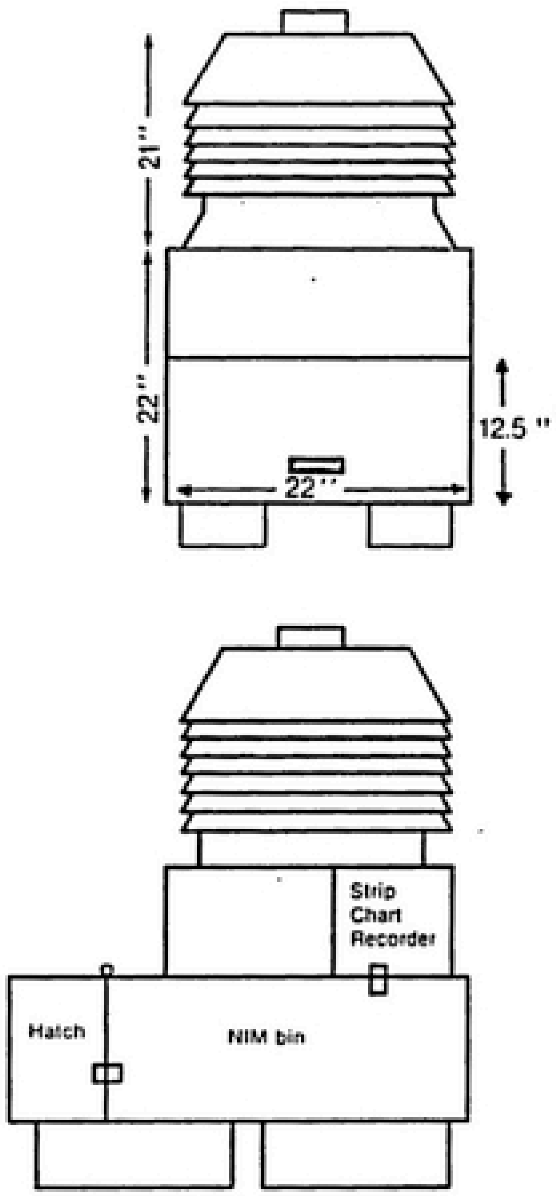

Figure 3. Electronics Housing

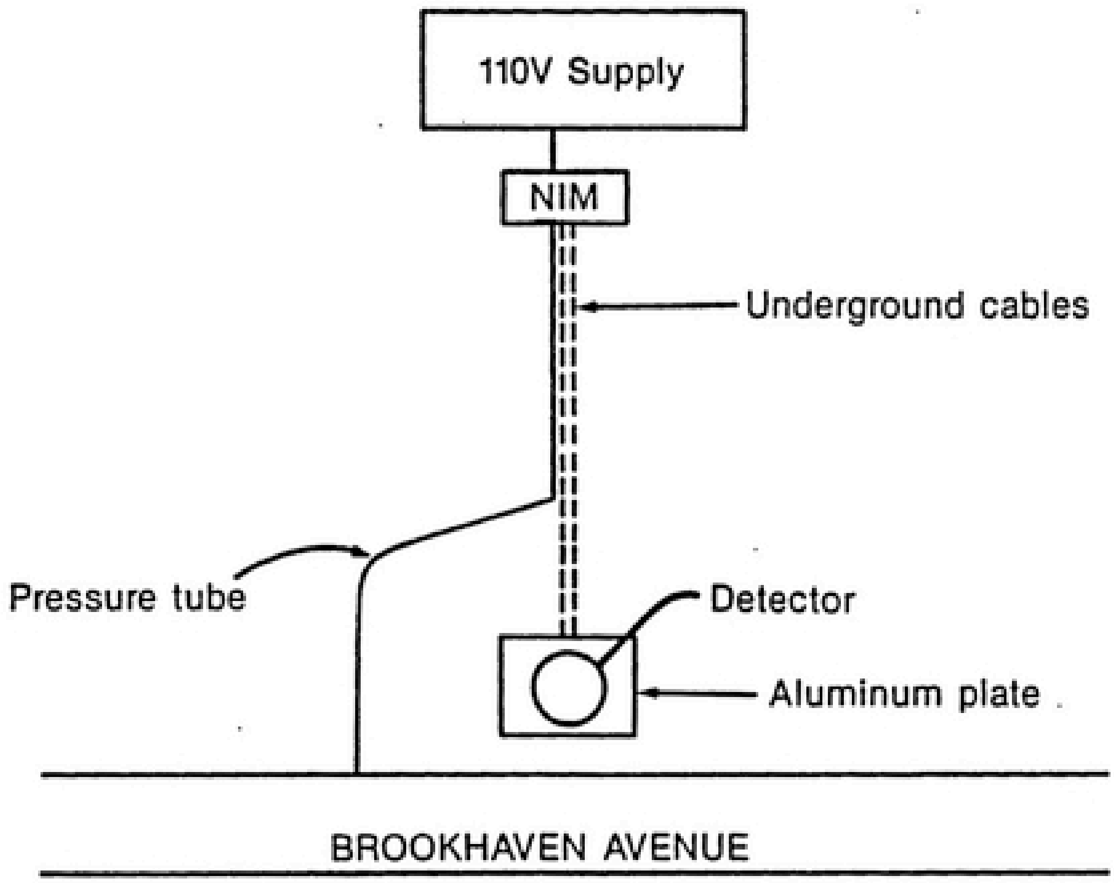

Figure 4. VPM Test Site

Nuclide	Activity (μCi)
^{133}Ba	8.96
^{137}Cs	10.36
^{60}Co	10.12
^{98}Y	5.08
^{22}Na	10.30
^{54}Mn	8.76
^{203}Hg	4.00

Additional sources used for testing were provided by the HP Instrumentation Shop and the Hot Lab at BNL. These sources were contained in large lead pigs because of their relatively high activity. The Brookhaven sources and the activity of each are listed below.

Nuclide	Activity (mCi)
^{192}Ir	66.0
^{137}Cs	0.6
^{60}Co	7.5

Monitoring Modality of System

The staff of the HP Instrumentation Shop equipped the VPM with the necessary circuitry to operate a monitoring modality activated by a signal from the pressure tube tripping device. This monitoring modality was designed to document the passage of a vehicle and record the level of radiation by the strip chart recorder as well as by the counter. This mode of operation is described as follows.

Barring a signal from the circuit, the system prints out hourly background counts around-the-clock to keep a reasonable check on background variability. When the pressure tube is tripped, the signal activates the strip chart recorder to run for a 10 second monitoring interval. The strip chart paper advances at a rate of 20 cm per minute and records the radiation level in counts per second as measured by the ratemeter.

At the same time, the signal from the pressure tube sends a pulse to the printer forcing a print-out of the accumulated background counts from the previous hourly print-out. The elapsed time since the last print-out is also recorded in the one second printing interval.

Following the background print-out, the system begins to count for two successive 4 second counting intervals, each of which is followed by a one second printing interval. During each printing interval the system ceases to count for one second.

The steps of the monitoring modality are given as follows:

1. Background print-out (1 sec) plus strip chart recorder begins 10 second monitoring interval.
2. First counting interval (4 sec).
3. Print-out (1 sec).
4. Second counting interval (4 sec).

5. Print-out (1 sec).

6. Return to hourly background counts.

At the end of 10 seconds the system returns to the hourly cycle of background counting. With the monitoring mode activated, further tripping of the pressure tube by the rear wheels is ignored.

Background Survey of Test Site

The detector head was buried about 30 feet from Bldg. 530 which once functioned as the Hot Machine Shop. The building remained posted for radioactivity and, therefore, it was necessary to perform a background survey of the area.

A survey meter responding in μR/hour, provided by the Calibration Shop, was used to survey the area around Bldg. 530 and the general vicinity of the VPM test site. Readings were taken at a height of 2 feet above ground. The results of this survey were recorded on a map of the site and showed the area to be within the range of background variability for the laboratory.

During the survey, a shipment of high level radioactive waste passed along Brookhaven Avenue destined for the Hazardous Waste Management Facility. At this time, the μR meter responded off-scale to the high level of radioactivity passing by the VPM test site.

It was recognized that the occasional high level waste shipments along Brookhaven Avenue would result in considerable elevation of background radiation at the test site. Such an elevation would be recorded by the hourly background counting modality of the VPM and would not present a problem unless the situation occurred simultaneously with the monitoring of a landfill refuse truck.

If, during the monitoring of a truck, a high level radioactive waste shipment were to pass by the test site, information regarding the presence or absence of low-level radioactivity in the refuse would be lost. The probability of such a coincidence, albeit low, would result in a spurious signal for activity in the refuse truck and yield a false positive reading for determining the percentage of refuse trucks shipping inadvertent radioactivity to the landfill.

The overall background radiation for the BNL site ranged from 8 to 20 μR/hr. The major portion of the area around the detector showed background levels of 8 to 10 μR/hr with only one point (next to Bldg. 530) showing a level of 20 μR/hr. The map of the test site in Figure 5 shows the values of the survey readings.

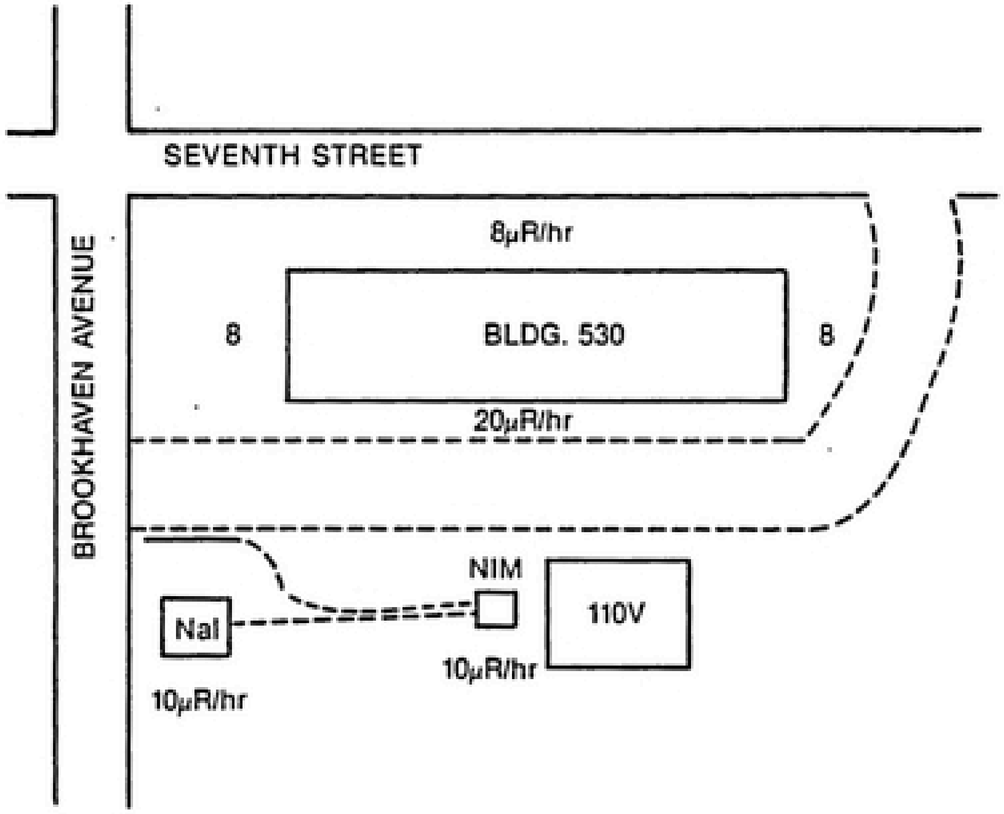

Figure 5. Background Survey of Test Site

Chapter III

TESTING PROCEDURES

Selection of Detector Size: Signal-to-Noise Ratio

The preliminary testing and assembly of the VPM was carried out at workbench space provided in the Calibration Shop at the laboratory. With the NIM bin electronics assembled at the workbench, the size of the NaI crystal to be used in the final assembly of the system was determined.

The decision for selection of crystal size was based on the criterion of signal-to-noise ratio which is an index of a crystal's ability to detect a radiation source in the presence of natural background radiation, assuming a sufficient signal size. This ratio was determined by the number of recorded counts from a reference source divided by the number of recorded counts from background radiation.

Three NaI crystals were available for testing. Each crystal was cylindrical in shape and coupled as a unit with a photomultiplier tube (PMT). The dimensions of each crystal were as follows:

1. 3 inches in diameter by 3 inches in height (3 X 3)
2. 4 inches in diameter by 2 inches in height (4 X 2)

3. 8 inches in diameter by 8 inches in height (8 X 8)

The procedure for obtaining data for the signal-to-noise ratio on each crystal was carried out as follows: A 4 μCi check source of ^{203}Hg was taped to a one inch thick aluminum block which was placed in contact with the crystal surface. The purpose of interposing one inch of aluminum between the source and the crystal was to simulate the field conditions of placing a one inch thick aluminum plate over the detector.

A series of five 10 second counts was made and recorded in average counts per second (cps). With the source removed, a series of five 10 second counts was made for background radiation. Background counts were also recorded in average cps. This procedure was followed for data collection on each of the three NaI crystals. During the counting procedure, each crystal was shielded from background by stacking lead bricks around the sides of the crystal.

The signal-to-noise test was repeated on the 3 x 3 inch crystal placed in the Baird well-counter lead pig.

Determination of Solid Angle of Detection

Solid angle of detection is defined as a three dimensional angle or solid cone, the apex of which is the face of the detector, subtended by the area of a plane parallel to the face of the detector within which a radiation source is detectable by the system. An isotropic source of radiation anywhere within the solid angle will elicit a response by the detector.

The purpose of determining the solid angle of detection of the VPM was to estimate the area in the bed of a truck that can be seen by the detector. Because of differences in placement of activity in a truck load and variability of paths taken by the passage of the vehicle over the detector, the solid angle of detection should be sufficient to detect a source located anywhere in the bed of a truck.

The method for determining the solid angle of detection is described as follows. The assembled detector head unit was oriented horizontally on the floor of the Calibration Shop. A 10 μCi source of ^{137}Cs was rolled on a dolly along a path (P) parallel to the face of the detector at a distance (d) of 100 cm at right angles to the face of the detector. A diagram of this geometry is given in Figure 6.

The diameter of the detection field along path (P) was determined in the following manner: Beginning the traverse of path (P), with the source outside the detection field, the ratemeter needle indicated a reading of background radiation at about 10 cps. As the source entered the detection field, a rapid response of the ratemeter needle above background was noted. This point (X), where the ratemeter began to show a response, was

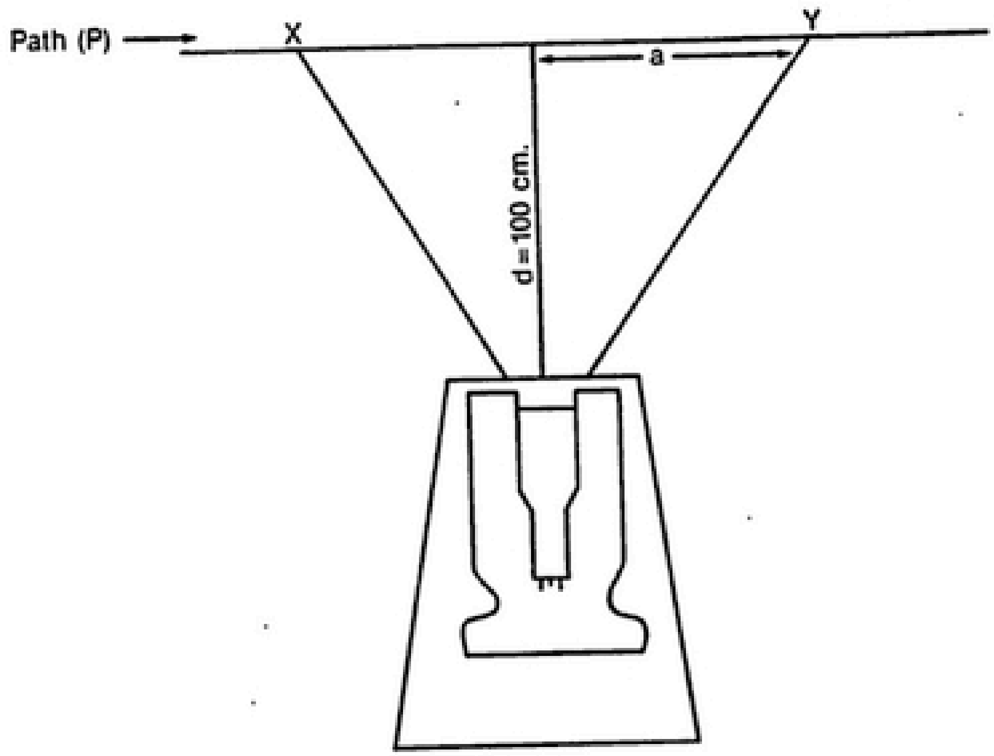

a=radius of detection field
d=source to detector distance a right angle

Figure 6. Solid Angle Geometry

marked by pencil on the floor of the shop to indicate the boundary of the detection field along path (P). The source was rolled further along path (P) with the ratemeter indicating continued response. When the ratemeter needle returned to its position for background this point (Y) was marked on the floor to indicate the opposite boundary of the field. Measurement between points X and Y determined the diameter of the detection field at 100 cm from the detector within which the system will respond to any activity present.

A distance of 100 cm corresponded to 39.3 inches between the measured detection field and the detector. With the bed of the test truck at a height of 30 inches from the buried detector, the measured detection field was 9.3 inches above the bed of the truck. The diameter of the detection field at this distance gave an indication of the area over the bed of the truck that can be seen by the detector.

The method for determining the solid angle of detection (Ω), in steradians, is given by the expression:

$$\Omega = 2\pi \left[1 - \frac{d}{\sqrt{d^2 + a^2}} \right] \quad \text{(Kn 79)}$$

where

d = source-to-detector distance at right angle to face of detector

a = radius of detection field

Determination of Dead Time

Dead time of a counting system is the minimum amount of time which must elapse between two events in order that they may be recorded as two separate pulses. Any event which occurs within the dead time of the system is lost from the total counting of true events, therefore, for precise measurement account must be made for dead time losses within the system. Dead time losses become greater with increasing interaction rates, thus affecting the ability of the system to measure high rates.

The method for determining the dead time (T) of a nonparalysable system was the Two-Source Method described in the NCRP Handbook of Radioactivity Measurements Procedures (NCRP 78). This method is based on observing the rates (n_1) and (n_2) from counting two sources individually, the combined source count rate (n_{12}) and the background rate (n_b).

Because the counting losses are non-additive, the observed rate from the combined sources (n_{12}) will be less than the sum of the rates observed for each source counted individually, ($n_1 + n_2$). Dead time can be calculated from the discrepancy using the following formula:

$$T = \{ 1- [1- (\Delta - n_b)\ q/p^2]^{\frac{1}{2}} \}\ p/q \qquad \text{(NCRP 78)}$$

where

$$\Delta = n_1 + n_2 - n_{12}$$

$$p = n_1 n_2 - n_b n_{12}$$
$$q = n_1 n_2 n_{12} + n_b(n_1 n_2 - n_1 n_{12} - n_2 n_{12})$$

Dead time of the VPM was determined at the test site using 10 μCi of ^{137}Cs and 10 μCi of ^{60}Co counted individually and in combination. Each count was made with the source(s) in direct contact with the protective aluminum plate over the detector. The source-to-detector distance was 3 inches.

The sequence of counting was ^{137}Cs, ^{60}Co and ^{137}Cs plus ^{60}Co which yielded observed rates n_1, n_2 and n_{12} respectively. Each rate was recorded in average cps determined from a series of five 30 second counts.

It should be noted that the determination of dead time at this time was made on the system which incorporated the Amp/Preamp component in the NIM bin electronics. This component was later replaced by the Amp/TSCA.

Determination of Linearity

Linearity is the ability of a counting system to measure accurately increasing interaction rates. An ideal system would show perfect linearity of measurement over a full range of rates. Because dead time losses are an inherent property of all systems, the deviation of the observed rate from the true rate widens as the interaction rate increases. To illustrate, a plot of observed rate (m) versus the true rate (n) is given in Figure 7. The

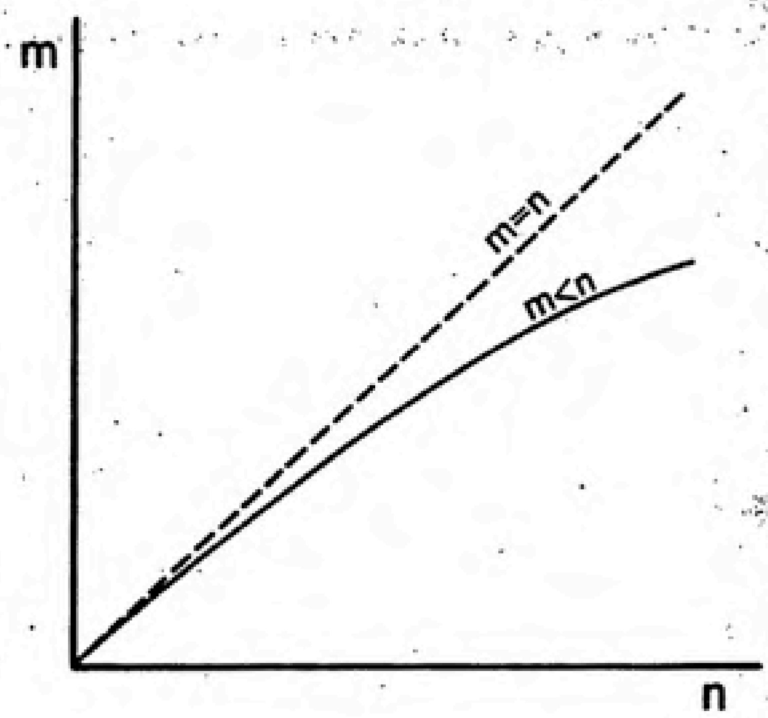

Figure 7. Variation of Observed Rate (m) as a Function of True Rate (n)

dashed linear curve represents the true count rate that would be observed with an ideal system. With no dead time losses m = n. Since losses due to dead time increase with higher interaction rates, the solid, non-linear curve represents the observed rate (m) as a function of true rate (n).

To determine the deviation from linearity of the VPM the following procedure was carried out at the test site on the original system using the Amp/Preamp. Three check sources were counted in contact with the aluminum plate which represented a source-to-detector distance of 3 inches. The three Amersham sources used in this procedure are listed below.

SOURCE	ACTIVITY
^{137}Cs	10 µCi
^{60}Co	10 µCi
^{54}Mn	8 µCi

Observed rates were recorded for each source, counted individually and in combination, by a series of five 30 second counts. The results of counting each individual source and combination of sources were recorded in average cps as was the background count rate.

The position for counting each source was carefully marked by pencil outline on the aluminum plate and the following counting sequence was performed:

COUNTING SEQUENCE

^{137}Cs

^{60}Co

^{54}Mn

$^{60}Co + ^{54}Mn$

$^{60}Co + ^{54}Mn + ^{137}Cs$

$^{137}Cs + ^{54}Mn$

$^{137}Cs + ^{60}Co$

Background

Values of theoretical count rates for each combination of sources were calculated by the summation of the observed net rates obtained from the individual counting of each source, assuming negligible dead time losses for single source counting. For example, the theoretical net rate for the combination of $^{60}Co + ^{54}Mn + ^{137}Cs$ was determined by summing the observed net rates for each of these sources counted singly. This procedure was repeated to obtain values of theoretical rates for all combinations of sources.

Determination of On-Vehicle Sensitivity

The sensitivity of a counting system is defined as the fraction of photon emissions that interacts with the detector crystal and is counted (NCRP 78). In this sense, the detection sensitivity is synonymous with the absolute efficiency of the system and is expressed as the number of counts/gamma.

On-vehicle sensitivity was determined for each photon energy by counting each source in a truck and dividing the observed net count rate by the photon emission rate of the source. The photon emission rate (gamma/minute) was determined from the activity (μCi) of the source, a conversion factor for the number of disintegrations per minute (dpm) per μCi and the photon emission probability per disintegration (gammas/disintegration). This method is given by the expression

$$\text{Gammas/min} = \text{activity } (\mu\text{Ci}) \times \frac{2.22 \times 10^6 \text{ dpm}}{\mu\text{Ci}} \times \text{gammas/disintegration.}$$

The expression for determining sensitivity is given by

$$\text{Sensitivity} = \frac{\text{observed net count rate (cpm)}}{\text{photon emission rate (gammas/min)}} = \text{counts/gamma.}$$

An experiment was designed to determine the on-vehicle sensitivity versus photon energy for the reference sources used. The design included the determination of sensitivity for each photon energy versus various thicknesses of sand attenuation on the truck.

On-vehicle sensitivity values were determined by counting the Amersham and Brookhaven sources on a stationary truck. The Brookhaven sources were used to determine sensitivity on the truck moving at 5 mph over the detector. These methods are presented in the following sections.

Stationary-Vehicle Sensitivity

The counting of each source in the bed of a stationary pickup truck was carried out at the VPM test site. The truck was parked over the detector with the rear axle and differential aligned directly over the detector head. Placement of each source was in line with the detector. Counting results for this alignment reflect the maximum inherent shielding of the truck since the differential presented the most attenuation material under the bed of the truck. The distance from the bed of the truck to the detector was 30 inches. Figure 8 shows the on-vehicle source alignment with the detector at the VPM test site.

Since any activity in a load of refuse may be shielded by other materials in the load, sensitivity for each source was determined for various additional attenuation conditions. The sources were counted at attenuation levels of 0, 3, 6, 9 and 12 inches of sand interposed between each source and the truck bed. A series of five 30 second counts was made for each source at each sand level in the truck. Background radiation was counted in the same manner. The Amersham sources were counted at five sand attenuation levels, while the Brookhaven sources were counted at 0, 6 and 12 inches of sand attenuation. The sand was contained in a cardboard box the dimensions of which were 13 x 9 x 13 inches.

Procedures for counting the Amersham and Brookhaven sources on the stationary truck and determination of the

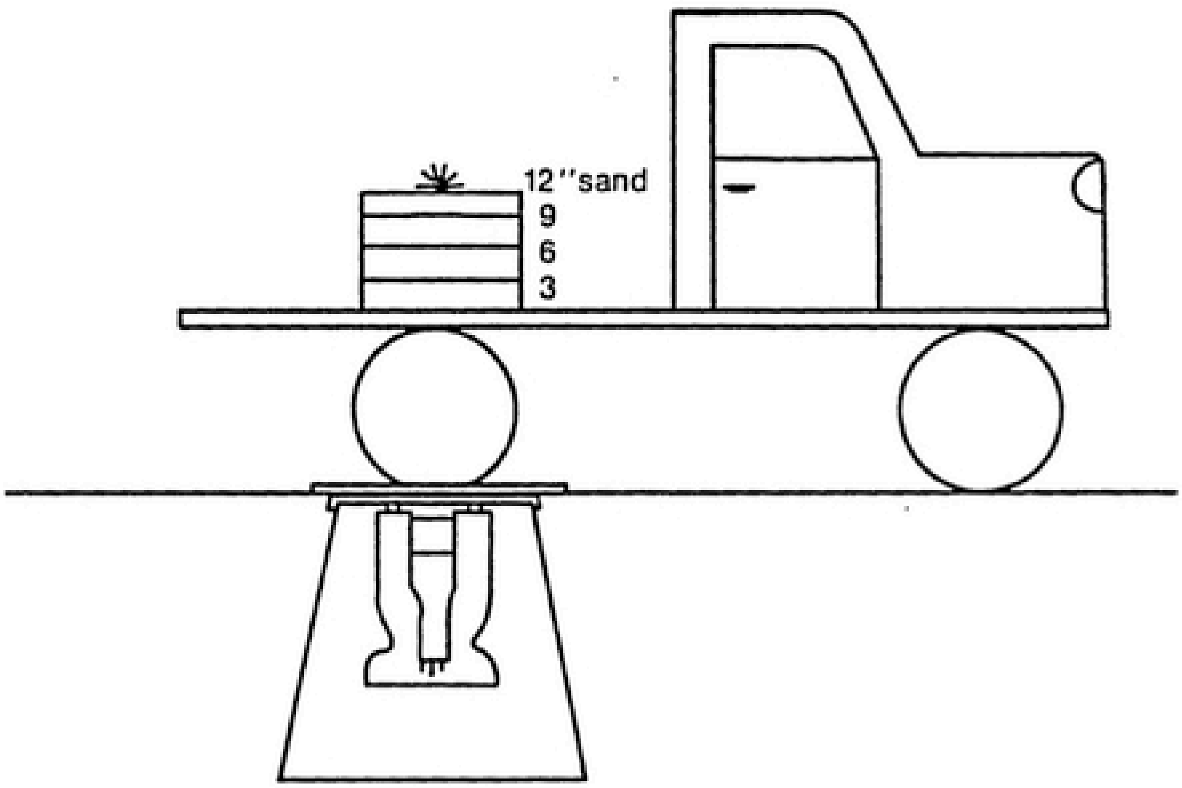

Figure 8. On-Vehicle Source Alignment at VPM Test Site

system's sensitivity for detecting these sources are given in the following sections.

Amersham Sources

The Amersham sources used for determining on-vehicle sensitivity are listed in Table 1, which includes the activity of each nuclide, the photon energy and photon emission probability per decay.

The activity of each nuclide was determined by calculating the remaining activity on the date of sensitivity testing using the original activity and the reference time listed on the certificate of measurement which accompanied the gamma reference source kit. The radioactive decay equation is given by

$$A_t = A_0 e^{-\lambda t}$$

where

A_t = activity remaining after a time interval t

A_0 = activity of nuclide measured at reference time

λ = decay constant for particular nuclide

t = elapsed time

e = base of natural logarithm: 2.718

It should be noted that since the several photon energies emitted by ^{133}Ba do not vary widely, no distinction was made among them. Hence, the assigned value for the photon energy of ^{133}Ba was a weighted average of all energies emitted. The same reasoning was

Table 1. Amersham Reference Sources

Nuclide	Activity (μCi)	Photon Energy (KeV)	Photon Emission Probability Per Decay (NCRP 78)
^{133}Ba	8.96	345*	0.98
^{137}Cs	10.36	662	0.85
^{54}Mn	8.76	834	1.00
^{60}Co	10.12	1250*	2.00
^{22}Na	10.30	1274 511	1.00 1.80
^{88}Y	5.08	898 1836	0.934 0.993

* weighted average of photon energies

applied to using a weighted average for the two energies emitted by ^{60}Co.

By a series of five 30 second counts, each Amersham source was counted in contact with the bed of the empty truck. The sources were then counted in contact with the surface of each sand level in the truck. Each sand level increased the source-to-detector distance (SDD) by increments of 3 inches. The SDD for each sand level is given below.

SAND LEVEL	SDD
0 inches	30 inches
3 inches	33 inches
6 inches	36 inches
9 inches	39 inches
12 inches	42 inches

The increased SDD made it necessary to determine distance correction factors to correct the averaged count rates of the Amersham sources for a uniform SDD. The rates were corrected to correspond to a source placement at 12 inches above the bed of the truck (SDD = 42 inches).

Distance correction factors were based on the inverse square law which states that the intensity of radiation varies inversely as the square of the distance from the source. The inverse square law is given mathematically as

$$I_2 = \frac{I_1}{d_2^{\,2}/d_1^{\,2}}$$

where

I_1 = intensity of radiation at d_1

I_2 = intensity of radiation at d_2

d_1 = SDD represented by height of truck bed (30 inches) plus incremental distance added by each level of sand

d_2 = SDD = 42 inches

The distance correction factors were determined by

$$d_2^{\,2}/d_1^{\,2}$$

and are given as follows

SAND LEVEL (inches)	DISTANCE CORRECTION FACTOR
0	$42^2/30^2 = 1.96$
3	$42^2/33^2 = 1.62$
6	$42^2/36^2 = 1.36$
9	$42^2/39^2 = 1.16$
12	$42^2/42^2 = 1.00$

The net count rates were distance corrected to a SDD of 42 inches by the expression

$$\text{Corrected net rate} = \frac{\text{gross rate} - \text{background}}{\text{distance factor}}$$

The corrected net counts/30 seconds were converted to counts/minute. Sensitivity for the photon energy of each Amersham source was determined by

$$\text{Sensitivity} = \frac{\text{corrected net rate (cpm)}}{\text{photon emission rate (gammas/minute)}}$$
$$= \text{counts/gamma}$$

This procedure determined the sensitivity of the VPM for the Amersham sources which reflected a source placement of 12 inches above the bed of the truck.

Brookhaven Sources

Stationary-vehicle sensitivity testing was repeated using the Brookhaven sources. Since these sources were of greater activity than the Amersham sources, they provided more statistically significant data. The particulars of the Brookhaven sources are listed in Table 2.

The activity of each Brookhaven source was determined by measuring the exposure rate in R/hr at one foot (30.48 cm) from each source with a survey meter due to a lack of documentation of source activity. Determination of activity from the exposure rate is given by the following equation:

Table 2. Brookhaven Reference Sources

Nuclide	Activity (mCi)	Photon Energy	Photon Emission Probability Per Decay
^{192}Ir	66.0	374 KeV*	2.08
^{137}Cs	0.6	662 KeV	0.85
^{60}Co	7.5	1250 KeV*	2.00

* weighted average of photon energies

$$Q = \frac{X\ d^2}{\Gamma}$$

where

Q = activity (mCi)

X = exposure rate (R/hr)

d = source-to-detector distance (cm)

Γ = gamma ray constant (R cm ^{2}/hr mCi) for the particular nuclide

Procedures for counting these sources on a stationary truck were similar to those previously described for the Amersham sources. The source and truck alignment remained the same. A series of five 30 second counts was recorded for each source. Sand levels of 0, 6 and 12 inches were interposed between each source and the bed of the truck. This time the position of each source was fixed at 12 inches above the bed of the truck to provide a uniform SDD of 42 inches.

The NIM bin electronics had been modified by the SEPD staff during the time between counting the Amersham sources and counting the Brookhaven sources. The Amp/Preamp used initially in the system had been replaced by the Amp/TSA. The effect of this change on the counting data will be discussed later.

Determination of sensitivity for gamma energies emitted by the Brookhaven sources was made using similar procedures to those previously described. The uniform SDD eliminated the need to distance correct the data.

Moving-Vehicle Sensitivity

An experiment was carried out to determine sensitivity by counting the Brookhaven sources in the pickup truck moving at 5 mph over the detector. Moving-vehicle counting data were recorded by driving the truck over the detector and tripping the pressure tube which activated the monitoring modality of the VPM.

The positioning of each source and the sand attenuation levels were the same as described previously, i.e. each source was taped at 12 inches above the bed of the truck and 0, 6 and 12 inches of sand were interposed between the source and the truck bed. With each source in place, the truck was driven at a speed of 5 mph over the detector. A series of five runs was made in this manner for each source at the various attenuation levels. Background data were recorded in the same manner.

The monitoring modality of the system recorded two 4 second counts for each run. The sources were actually seen by the detector only during the first 4 second counting interval since the truck was well beyond the detector by the time of the second 4 second count.

Each series of counts/4 seconds for each source was averaged and recorded as average gross counts/4 seconds. The average background count rate was subtracted from each gross count rate to determine the average net counts/4 seconds.

Moving-vehicle sensitivities for photon energies of these sources were determined by converting each net rate to counts per second and dividing by the photon emission rate in gammas/second. The resulting sensitivity values for the photon energy of each source on a moving vehicle were recorded in counts/gamma.

Determination of Lower Limits of Detection

To estimate the amount of a radionuclide that could escape detection by the VPM it was necessary to determine the lower limits of detection (LLD), also referred to as the minumum detectable activity (MDA) for each nuclide. The net count rates recorded for the Amersham and Brookhaven sources were used for this determination.

LLD has been defined by Pasternack as "the smallest amount of sample activity that will yield a net count for which there is a confidence at a predetermined level that activity is present" (Co 80). Determination of the LLD is related to the characteristics of the counting system and is based on statistical hypothesis testing for the presence of activity. Since the LLD is derived statistically, the use of the term does not denote an absolute level of activity that can or cannot be detected, but rather it serves as a guide for approximating the minimum level of activity that may be detected with confidence (NCRP 78).

Hypothesis testing is a form of decision process whereby sample data are assembled to produce a value that leads to a choice between two decisions, i.e., accept or reject the hypothesis (Re 70). In the case of the LLD, the choice is between accepting a value of net counts as a true signal for detection of activity, or rejecting this value as non-detection of activity.

In such a decision process, one can never be absolutely certain that the correct choice was made because of two types of error inherent in hypothesis testing. Currie describes Type I error as deciding that activity is present when it is not. The probability of making a Type I, false detection error is given by α. Type II error is described as failing to decide that activity is present when it is. The probability of making a Type II, false non-detection error is given by β. Since the probability for both types of error should be kept low, it is customary to accept a level of tolerance for both α and β equal to 0.05 (Co 80) (NCRP 78) (Cu 68).

In any discussion of LLD two terms, Critical Limit (L_C) and Detection Limit (L_D), must be defined. L_C is the number of net counts which must be exceeded to yield a decision of "detected". It is established a posteriori from the data at hand by the acceptable value for α together with the standard deviation, s_o, of the net signal when the mean of the net counts equal zero. Such a sample count is analogous to background counts. Mathematically L_C is given as

$$L_C = k_\alpha s_o \qquad \text{(Cu 68)}$$

where

k_α = upper percentile of the standardized normal variate corresponding to $\alpha = 0.05$.

s_o = standard deviation of the sample when the mean of the net counts is equal to zero (Standard deviation of background counts).

L_D is the signal level such that the number of net counts at or above this level is likely to be detected. It is established a priori by specifying the L_C, the acceptable probability for false non-detection β and the standard deviation of net counts when the mean of the net counts equals the L_D. Mathematically, the detection limit is given as

$$L_D = L_C + k_\beta s_D = k_\alpha s_o + k_\beta s_D \qquad \text{(Cu 68)}$$

where

k_β = upper percentile of the standardized normal variate corresponding to $\beta = 0.05$.

s_D = standard deviation of the signal when the mean of the net counts equals the L_D.

The L_D is synonymous with the LLD and is the signal level such that a signal at or above this level is likely to be detected with confidence.

Currie has shown that, with equal values of α and β such that $\alpha = \beta = 0.05$, the expression for the L_D is given as

$$L_D = k^2 + 2\sqrt{2}\, ks_b = 2.71 + 4.65\, s_b \qquad \text{(Cu 68)}$$

where

k_α = 1.64: the value of the standardized normal deviate corresponding to the preselected risk for $\alpha = 0.05$.

s_b = standard deviation of background counts.

The working expression used for determining the LLD for the VPM is given by:

$$LLD = C\,(2.71 + 4.65\, s_b) \qquad \text{(Co 80)}$$

where

C = proportionality constant relating the detector response to the activity, such as C = 1/e where e is the number of net counts per μCi.

s_b = standard deviation of background counts.

Values of LLD for each nuclide were determined from the same counting data as were used for sensitivity determination.

Chapter IV

RESULTS

Signal-to-Noise Ratio

Results of signal-to-noise testing for selection of crystal size used in the assembly of the VPM are presented in Table 3.

Table 3. Signal-to-Noise Ratio

CRYSTAL SIZE	SIGNAL TO NOISE RATIO
8 x 8 inch	15
4 x 2	53
3 x 3	59
3 x 3 in pig	421

According to the findings, the 8 x 8 inch crystal showed the lowest signal-to-noise ratio. This relatively low result was due to the fact that the large dimensions of this crystal increased the level of noise faster than that of the signal. In addition, the dimensions of the 8 x 8 made shielding more difficult.

The higher values of signal-to-noise ratio for the 4 x 2 inch and the 3 x 3 inch crystals demonstrated their greater effectiveness in detecting a radiation source in the presence of background. Results of testing the smaller crystals showed their signal-to-noise performance to be comparable. The ratio for the 3 x 3 inch crystal, however, was greatly increased when it was tested in the well of the Baird lead pig. The factor contributing to this improvement was the excellent shielding from background radiation afforded by the several inches of lead surrounding the sides of the crystal.

The Baird lead pig not only improved the signal-to-noise ratio of the 3 x 3 inch crystal but also provided excellent protection from environmental conditions encountered by the detector buried at the test site. These advantages were the decisive factors for selection of the 3 x 3 inch crystal to be used in the final assembly of the system.

Solid Angle of Detection

Solid angle of detection for the detector head was determined by measuring the distance between points X and Y which marked the boundaries of the detection field at a distance of 100 cm from the face of the detector. The diameter of this field was measured to be 210 cm. A diagram of the solid angle dimensions is given in Figure 9.

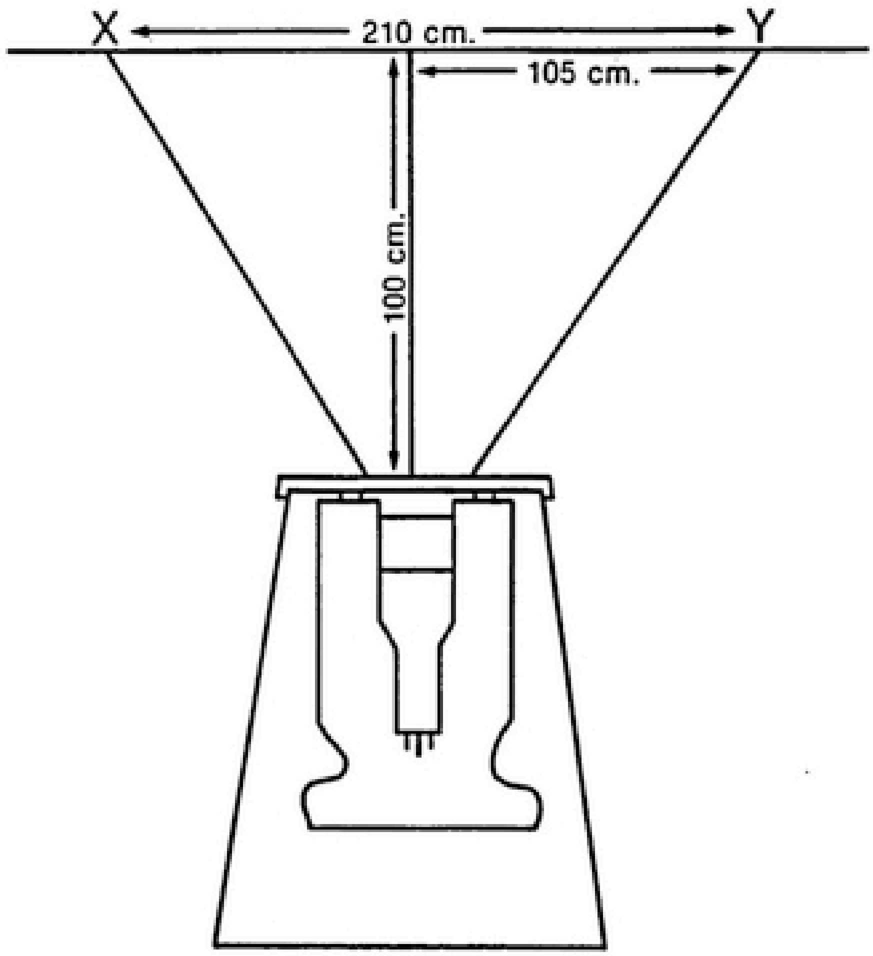

Figure 9. Dimensions of Solid Angle Geometry

The solid angle of detection was determined to be 1.9 steradians by the expression

$$\Omega = 2\pi\left[1 - \frac{100\ \text{cm}}{\sqrt{100\ \text{cm}^2 + 105\ \text{cm}^2}}\right] = 1.9\ \text{steradians}$$

(Kn 79)

The distance of 100 cm from the detector, at which the detection field was measured, corresponded to 39.3 inches. With the height of the truck bed at 30 inches above the buried detector, the measured detection field was 9.3 inches above the bed of the truck. The 210 cm diameter of the detection field corresponds to 6.8 feet which was the diameter of the area at 9.3 inches above the bed of the truck that could be seen by the detector.

Dead Time

Results of the two-source method for dead time determination are given below.

Average gross count rates observed for the counting of ^{137}Cs and ^{60}Co individually and in combination are presented below as is the average background count rate.

NUCLIDE	OBSERVED GROSS COUNT RATE (CPS)
^{137}Cs (n_1)	7361
^{60}Co (n_2)	16252
^{137}Cs + ^{60}Co (n_{12})	22794
Background (n_b)	10

The dead time of the VPM was determined to be 3.5 microseconds using the previously described formula

$$T = \{ 1 - [1 - (\Delta - n_b)\ q/p^2]^{\frac{1}{2}}\}\ p/q \qquad \text{(NCRP 78)}$$

This dead time was determined for the original system which incorporated the Amp/Preamp in the NIM bin electronics.

Linearity

Table 4 lists the results of counting procedures for determining deviation from linearity of the original VPM system. The count rate for each single source as well as each combination of sources counted is listed with the corresponding observed gross rate, observed net rate and the theoretical net rate. Theoretical rates for combination counts were determined by the summation of the observed net rates obtained from the single counting of each source within the combination.

Since the observed rates for the combination counts were less than the determined theoretical rates, the plot of observed rates versus theoretical rates, given in Figure 10, shows the original system's deviation from linearity due to dead time losses. The dashed curve for the observed rates demonstrates that the discrepancy widens with increasing interaction rate.

Table 4. Linearity Test Results

Sources	Observed Gross Count Rate (cps)	Observed Net Count Rate (cps)	Theoretical Net Count Rate (cps)
^{54}Mn	7120	7110	7110
^{137}Cs	7361	7351	7351
^{60}Co	16252	16242	16242
^{60}Co + ^{54}Mn	22557	22547	23352
^{60}Co + ^{137}Cs	22794	22784	23593
^{54}Mn + ^{137}Cs	14086	14076	14461
^{54}Mn + ^{137}Cs + ^{60}Co	28769	28759	30703
Background	10		

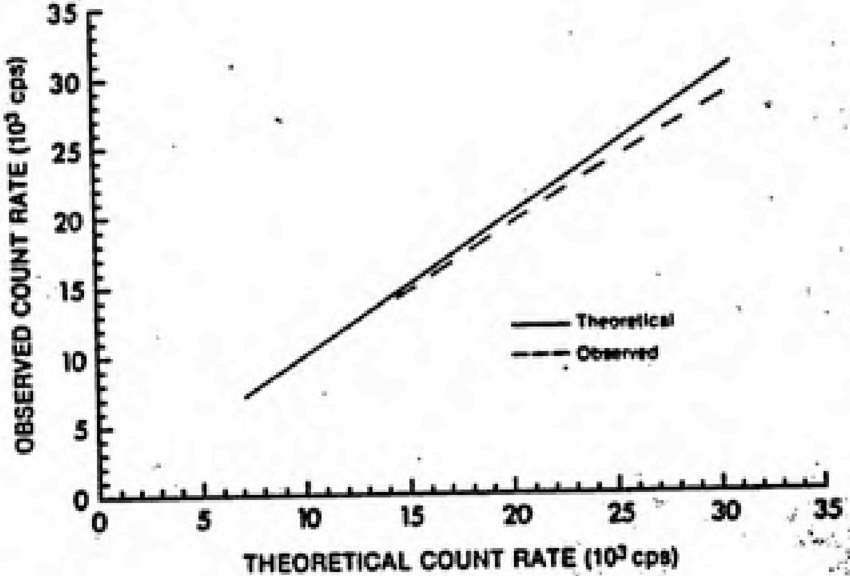

Figure 10. Linearity of Detector

Sensitivity

Determination of on-vehicle sensitivity was made by recording count rates for the Amersham and Brookhaven sources at various sand attenuation levels on the truck parked over the detector head. Moving-vehicle sensitivity was determined by recording count rates for the Brookhaven sources on the truck traveling at 5 mph over the detector. Results of counting procedures for stationary and moving-vehicle sensitivity are given in the following sections.

Stationary-Vehicle Sensitivity

Amersham Sources

Sensitivity versus photon energy was determined for each of the Amersham sources counted at five sand attenuation levels on the stationary truck. The following tables present the results of counting procedures and sensitivity for the Amersham sources.

Table 5 lists the average gross counts/30 seconds observed for each nuclide counted at each sand attenuation level on the truck. The background rate was an overall average of background counts for each sand attenuation level. This was used to determine net rates because background did not vary widely with incremental increases in sand attenuation.

Table 6 gives the net count rates per 30 seconds, distance corrected to reflect source placement at 12 inches above the bed of the truck. Distance corrected net

Table 5. On-vehicle Gross Counts/30 Seconds, Amersham Sources

Nuclide	0" Sand	3" Sand	6" Sand	9" Sand	12"Sand
^{133}Ba	459 ± 30	359 ± 22	299 ± 15	297 ± 21	326 ± 33
^{137}Cs	732 ± 30	522 ± 36	408 ± 21	353 ± 21	332 ± 31
^{54}Mn	808 ± 22	631 ± 51	478 ± 23	388 ± 46	344 ± 22
^{22}Na	1883 ± 66	1169 ± 18	706 ± 36	540 ± 30	464 ± 25
^{60}Co	2043 ± 66	1369 ± 31	926 ± 25	600 ± 41	515 ± 27
^{88}Y	1181 ± 16	899 ± 25	603 ± 37	493 ± 37	400 ± 18

Background = 292 (19) counts/30 sec.

Table 6. On-Vehicle Net Counts/30 Seconds*, Amersham Sources

Nuclide	0" Sand	3" Sand	6" Sand	9" Sand	12" Sand
^{133}Ba	85 ± 25	41 ± 23	**	**	**
^{137}Cs	224 ± 25	142 ± 32	85 ± 24	53 ± 26	40 ± 36
^{54}Mn	263 ± 20	209 ± 43	137 ± 26	83 ± 46	52 ± 29
^{22}Na	812 ± 49	541 ± 21	304 ± 35	213 ± 33	172 ± 31
^{60}Co	893 ± 49	665 ± 29	466 ± 27	266 ± 42	223 ± 33
^{88}Y	454 ± 18	375 ± 25	229 ± 36	173 ± 39	108 ± 26

* distance corrected to 12" above bed

** statistically insignificant net count rates count rates were determined by subtracting background from the gross rates and dividing the remainder by a distance factor. The expression for this determination is given by

$$\text{Net rate} = \frac{\text{gross - background}}{\text{distance factor}}$$

where the distance factor at

0" sand = 1.96

3" sand = 1.62

6" sand = 1.36

9" sand = 1.16

12" sand = 1.00

Table 7 shows the distance corrected net rates in counts/minute which were determined by doubling the net counts/30 seconds. These values were used to determine the sensitivity for photon energies emitted by each of the nuclides.

Table 8 presents the values of sensitivity versus photon energies of the Amersham sources used in stationary vehicle testing of the VPM. Values of sensitivity are expressed in 10^{-5} counts/gamma and were determined by dividing the net count rate (cpm) by the photon emission rate (gpm) for each gamma energy emitted (See Appendix I).

Brookhaven Sources

Sensitivity testing for the stationary vehicle was repeated by counting the Brookhaven sources with 0, 6 and

Table 7. On-Vehicle Net Counts/Minute*, Amersham Sources

Nuclide	0" Sand	3" Sand	6" Sand	9" Sand	12" Sand
^{133}Ba	170 ± 50	82 ± 46	**	**	**
^{137}Cs	448 ± 50	284 ± 64	170 ± 48	106 ± 52	80 ± 72
^{54}Mn	526 ± 40	418 ± 86	274 ± 52	166 ± 92	104 ± 58
^{22}Na	1624 ± 98	1082 ± 42	608 ± 70	426 ± 66	344 ± 62
^{60}Co	1786 ± 98	1330 ± 58	932 ± 54	532 ± 42	446 ± 66
^{88}Y	908 ± 36	750 ± 50	458 ± 72	346 ± 78	216 ± 92

* distance corrected to 12" above bed

** statistically insignificant net count rates

Table 8. On-Vehicle Sensitivity (10^{-5} Counts/Gamma) vs. Photon Energy, Amersham Sources

Energy (KeV)	0" Sand	3" Sand	6" Sand	9" Sand	12" Sand
345	0.87 ± 0.26	0.42 ± 0.24	**	**	**
511	1.73 ± 0.27	0.98 ± 0.13	0.32 ± 0.18	0.38 ± 0.17	0.28 ± 0.17
662	2.30 ± 0.26	1.46 ± 0.33	0.87 ± 0.25	0.54 ± 0.27	0.41 ± 0.37
834	2.71 ± 0.21	2.15 ± 0.44	1.41 ± 0.27	0.86 ± 0.47	0.54 ± 0.30
898	2.71 ± 0.21	2.15 ± 0.44	1.41 ± 0.27	0.86 ± 0.47	0.54 ± 0.30
1250	3.98 ± 0.22	2.96 ± 0.13	2.08 ± 0.12	1.18 ± 0.10	0.99 ± 0.15
1274	3.98 ± 0.22	2.96 ± 0.13	2.08 ± 0.12	1.18 ± 0.10	0.99 ± 0.15
1836	5.57 ± 0.38	4.69 ± 0.61	2.77 ± 0.69	2.29 ± 0.82	1.42 ± 0.87

** statistically insignificant sensitivity values

12 inches of sand attenuation in the truck. The reason for the repetition was to provide more statistically significant net count rates for low energy photons at the higher attenuation levels. The higher activities of the Brookhaven sources did yield more meaningful results for all data points. The 66 mCi source of ^{192}Ir, which emits an average photon energy of 374 KeV, was used in place of ^{133}Ba (345 KeV) for low energy sensitivity determination because a mCi source of ^{133}Ba was not available.

Results of counting the Brookhaven sources on the stationary truck are given in the following tables. Table 9 lists the average gross counts/30 seconds for each of the sources counted at three sand attenuation levels with a fixed source placement at 12 inches above the bed of the truck (SDD = 42 inches). The background count rate is an overall average value.

Table 9. Stationary-Vehicle Gross Counts/30 Seconds Brookhaven Sources

Nuclide	0" Sand	6" Sand	12" Sand
^{192}Ir	1066641 ± 10450	348880 ± 1853	118444 ± 698
^{137}Cs	13145 ± 73	5734 ± 64	2042 ± 40
^{60}Co	389209 ± 744	233811 ± 1028	120264 ± 419

Background 209 (14)

Table 10 gives the average net counts/30 seconds which were determined by subtracting background from each gross count rate.

Table 10. Stationary-Vehicle Net Counts/30 Seconds, Brookhaven Sources

Nuclide	0" Sand	6" Sand	12" Sand
^{192}Ir	1066432 ± 10450	348671 ± 1853	118235 ± 698
^{137}Cs	12936 ± 74	5525 ± 66	1833 ± 42
^{60}Co	389000 ± 744	233602 ± 1028	120055 ± 419

Table 11 gives the net rates for each source in counts/minute. These values were determined by doubling the net counts/30 seconds.

Table 11. Stationary-Vehicle Net Counts/Minute, Brookhaven Sources

Nuclide	0" Sand	6" Sand	12" Sand
^{192}Ir	2132864 ± 20900	697759 ± 3706	236471 ± 1395
^{137}Cs	25872 ± 149	11050 ± 131	3666 ± 85
^{60}Co	778000 ± 1488	467204 ± 2056	240110 ± 838

Sensitivity values (10^{-5} counts/gamma) for photon energies emitted by the Brookhaven sources are presented in Table 12.

Because of the higher emission rates of the Brookhaven sources and the modification of the system by substituting the Amp/TSCA for the Amp/Preamp, it was necessary to determine sensitivity for the Brookhaven sources from dead time corrected count rates. The dominant dead time of the modified system with the Amp/TSCA was 16 μsec (Bi 85).

Net count rates for the Brookhaven sources were corrected for the increased dead time by the expression

$$N = \frac{n}{(1 - nT)} - \text{background}$$

where

N = true interaction rate

n = observed rate

T = dead time of 16 μsec.

Sensitivity for the higher activity sources was then determined from the corrected net count rates by the following method.

$$\text{Sensitivity} = \frac{\text{Corrected net count rate (cps)}}{\text{photon emission rate (gps)}}$$

Dead time corrected net count rates for the Brookhaven sources counted on a stationary truck are given in Table 13.

Table 12. Stationary-Vehicle Sensitivity (10^{-5} Counts/Gamma) vs. Photon Energy, Brookhaven Sources.

Nuclide	Energy (KeV)	0" Sand	6" Sand	12" Sand
^{192}Ir	374	0.70 ± 0.006	0.23 ± 0.0012	0.08 ± 0.00045
^{137}Cs	662	2.29 ± 0.013	0.98 ± 0.012	0.32 ± 0.0075
^{60}Co	1250	2.34 ± 0.0047	1.40 ± 0.0062	0.72 ± 0.0025

Table 13. Dead Time Corrected Net Count Rates (cps) for Brookhaven Sources on Stationary Vehicle

Nuclide	0" Sand	6" Sand	12" Sand
^{192}Ir	82464 ± 1337	14280 ± 78	4207 ± 25
^{137}Cs	434 ± 2.5	185 ± 2.2	61 ± 1.4
^{60}Co	16366 ± 33	8897 ± 39	4276 ± 15

Sensitivity values determined from dead time corrected net count rates for the Brookhaven sources are given in Table 14.

Moving-Vehicle Sensitivity

Moving-vehicle sensitivity was determined by counting each of the Brookhaven sources on the truck moving at 5 mph over the detector. Count rates for these nuclides were recorded during the 4 second counting interval activated by a signal from the pressure tube tripping device. Sensitivity values reflect source placement at 12 inches above the bed of the truck with the interposition of three sand attenuation levels between the source and the detector. Results of this counting procedure are given in the following tables.

Table 15 lists the average gross rates in counts/4 seconds for each source at various attenuation levels. The background count rate was an overall average value.

Table 14. Dead Time Corrected Sensitivity (10^{-5} Counts/Gamma) for Brookhaven Sources on Stationary Vehicle

Nuclide	Energy (KeV)	0" Sand	6" Sand	12" Sand
^{192}Ir	374	1.62 ± 0.026	0.28 ± 0.0015	0.08 ± 0.00049
^{137}Cs	662	2.30 ± 0.013	0.98 ± 0.016	0.32 ± 0.0074
^{60}Co	1250	2.95 ± 0.0059	1.60 ± 0.0070	0.77 ± 0.0027

Table 15. Moving-Vehicle Gross Counts/4 Seconds, Brookhaven Sources

Nuclide	0" Sand	6" Sand	12" Sand
^{192}Ir	91295 ± 9148	69067 ± 5701	22943 ± 1742
^{137}Cs	1468 ± 209	923 ± 56	326 ± 37
^{60}Co	43052 ± 1868	25099 ± 1366	12657 ± 2987

Background 34 ± 2

Table 16 gives the average net counts/4 seconds determined by subtracting background from each gross rate.

Table 16. Moving-Vehicle Net Counts/4 Seconds, Brookhaven Sources

Nuclide	0"Sand	6" Sand	12" Sand
^{192}Ir	91261 ± 9148	69033 ± 5701	22943 ± 1742
^{137}Cs	1434 ± 209	889 ± 56	292 ± 37
^{60}Co	43018 ± 1868	25065 ± 1366	12623 ± 2987

Table 17 gives the net count rates in counts/second which were determined by dividing the net counts/4 second by 4.

Table 17. Moving-Vehicle Net Counts/Second, Brookhaven Sources

Nuclear	0"Sand	6" Sand	12" Sand
^{192}Ir	22814 ± 2287	17258 ± 1425	5727 ± 435
^{137}Cs	358 ± 52	222 ± 14	73 ± 9
^{60}Co	10754 ± 467	6266 ± 342	3155 ± 747

Table 18 presents moving-vehicle sensitivity versus photon energy of the Brookhaven sources determined by the quotient of net counts/second and the photon emission rate of each source in gammas/second.

Dead time corrected sensitivities for the Brookhaven sources counted on a moving vehicle are presented in Table 19.

Lower Limits of Detection

LLD values (μCi) presented in this section were determined from counting data obtained at the VPM test site. LLD values are listed for the Amersham and Brookhaven sources counted on a stationary vehicle and for the Brookhaven sources counted on a moving vehicle. All values represent a source placement at 12 inches above the bed of the truck.

Table 20 gives LLD values for the Amersham sources counted at five attenuation levels on a stationary vehicle.

Table 18. Moving-Vehicle Sensitivity (10^{-5} Counts/Gamma) vs. Photon Energy, Brookhaven Sources

Nuclide	Energy (Kev)	0" Sand	6" Sand	12" Sand
^{192}Ir	374	0.45 ± 0.05	0.34 ± 0.03	0.11 ± 0.0086
^{137}Cs	662	1.89 ± 0.28	1.17 ± 0.07	0.39 ± 0.05
^{60}Co	1250	1.94 ± 0.08	1.13 ± 0.06	0.57 ± 0.13

Table 19. Dead Time Corrected Sensitivity (10^{-5} Counts/Gamma) for Brookhaven Sources on Moving Vehicle.

Nuclide	Energy (KeV)	0" Sand	6" Sand	12" Sand
^{192}Ir	374	0.71 ± 0.082	0.47 ± 0.042	0.12 ± 0.010
^{137}Cs	662	1.90 ± 0.28	1.18 ± 0.074	0.39 ± 0.048
^{60}Co	1250	2.34 ± 0.10	1.26 ± 0.069	0.60 ± 0.14

Table 20. Lower Limits of Detection (μCi) on Stationary Vehicle, Amersham Sources

Nuclide	0" Sand	3" Sand	6" Sand	9" Sand	12" Sand
^{133}Ba	9.60 ± 2.82	19.90 ± 11.16	**	**	**
^{137}Cs	4.21 ± 0.47	6.64 ± 1.50	11.10 ± 3.13	17.80 ± 8.73	23.58 ± 21.23
^{54}Mn	3.03 ± 0.23	3.82 ± 0.79	5.82 ± 1.11	9.61 ± 5.33	15.34 ± 8.56
^{22}Na	1.16 ± 0.07	1.73 ± 0.07	3.09 ± 0.36	4.40 ± 0.68	5.45 ± 0.98
^{60}Co	1.03 ± 0.06	1.39 ± 0.06	1.98 ± 0.11	3.46 ± 0.55	4.13 ± 0.61
^{88}Y	1.02 ± 0.04	1.23 ± 0.08	2.02 ± 0.32	2.67 ± 0.60	4.28 ± 1.03

** statistically insignificant values

Lower limits of detection for the Brookhaven sources counted on the stationary and moving vehicle were determined from the dead time corrected net count rates for these sources.

Table 21 presents the results of LLD determined for the Brookhaven sources counted on a stationary vehicle.

Table 21. Lower Limits of Detection (μCi) on Stationary Vehicle, Brookhaven Sources (Dead Time Corrected Values)

Nuclide	0" Sand	6" Sand	12" Sand
^{192}Ir	1.81 ± 0.029	10.45 ± 0.057	35.46 ± 0.207
^{137}Cs	3.12 ± 0.018	7.33 ± 0.087	22.23 ± 0.51
^{60}Co	1.04 ± 0.0021	1.91 ± 0.0083	3.96 ± 0.014

Table 22 gives the results of LLD determined for the Brookhaven sources counted on a vehicle moving at 5 mph over the detector.

Table 22. Lower Limits of Detection (μCi) on Moving Vehicle Brookhaven Sources (Dead Time Corrected Values)

Nuclide	0" Sand	6" Sand	12" Sand
^{192}Ir	5.51 ± 0.64	8.31 ± 0.73	31.42 ± 2.61
^{137}Cs	5.00 ± 0.72	8.11 ± 0.51	24.68 ± 3.13
^{60}Co	1.73 ± 0.08	3.23 ± 0.18	6.78 ± 1.61

Chapter V

DISCUSSION

On-vehicle sensitivity results and LLD values determined for the VPM are presented graphically in the following sections. The curves show the trends in these performance parameters and allow for comparison of performance by the system under different conditions such as moving-vehicle versus stationary-vehicle results.

Sensitivity Curves for Amersham Sources

On-vehicle sensitivity performance of the VPM determined from data collected for the Amersham sources on a stationary truck is plotted in Figure 11. Photon energies emitted by these sources ranged from 345 to 1836 KeV.

The curves show an upward trend of sensitivity with increasing photon energy. Transmission of photons through matter depends on the atomic number of the absorber and the energy of the gamma radiation (Ce 83). Intensity of gamma radiation transmitted is proportional to the energy of the primary photons. Therefore, the sensitivity of the system is proportional to the photon energy of each nuclide.

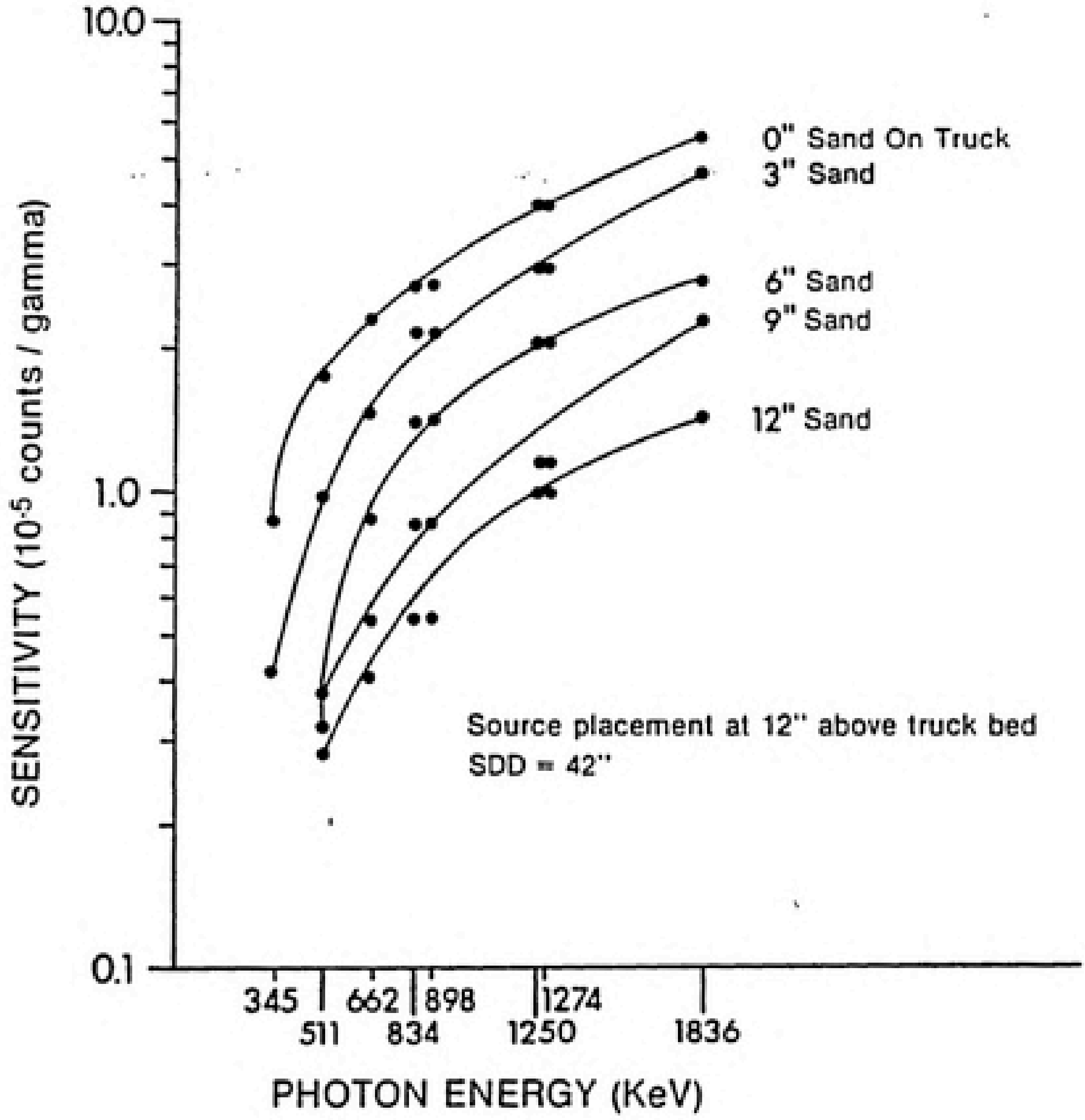

Figure 11. On-Vehicle Sensitivity Curves, Amersham Sources on Stationary Vehicle

The curves also show the reduction in sensitivity over all energies with incremental increases in absorber thickness. Each sand attenuation level in the truck, interposed between the source and the detector, increased the absorption of photons of all energies. Photon interaction with the NaI crystal, and hence the sensitivity, is inversely proportional to the level of sand attenuation. Attenuation differences more than offset sensitivity drop with increases in energy.

Curves for the Amersham sources show the loss of sensitivity at the low energy range for attenuation levels of 6 or more inches of sand. This was due to the lack of statistically significant net count rates observed for ^{133}Ba when counted at higher attenuation levels. The greater attenuation was sufficient to absorb most of the 345 KeV photons thus preventing their interaction with the NaI crystal. The low activity of the ^{133}Ba source (8.96 μCi), the source-to-detector distance and the high attenuation levels were the factors contributing to the inability to determine sensitivity at the low energy range. For this reason, sensitivity curves for 6, 9 and 12 inches of sand do not extend down to the 345 KeV energy level indicating a limitation of the system's response.

Sensitivity Curves for Brookhaven Sources

Sensitivity curves for the Brookhaven sources counted on both the stationary and moving truck at attenuation levels of 0, 6 and 12 inches of sand are presented in Figure 12. Photon energies for these sources range from 374 to 1250 KeV.

The mCi amounts of the Brookhaven sources yielded statistically meaningful counting results over the entire energy range at all attenuation levels. For this reason, the ability to determine sensitivity for low energy photons was demonstrated by all curves on the graphs for both the stationary and moving vehicle.

Stationary-vehicle sensitivity curves given in Figure 12 (a) show the upward trend of the system's response with increasing photon energy at all attenuation levels. Moving-vehicle sensitivity curves, shown in Figure 12 (b), demonstrate the general upward trend of sensitivity.

Sensitivity values for the Brookhaven sources on both the stationary and moving truck were corrected for dead time losses and are discussed in the following section on comparison of sensitivity findings.

Comparison of Sensitivity Findings

Comparison of stationary-vehicle sensitivities for the Amersham and Brookhaven sources is presented in Figure 13. The system's response to μCi sources of ^{133}Ba, ^{137}Cs and ^{60}Co is compared with that for mCi sources of ^{192}Ir, ^{137}Cs and ^{60}Co.

Generally, the Brookhaven sources yielded more statistically significant sensitivity values because of

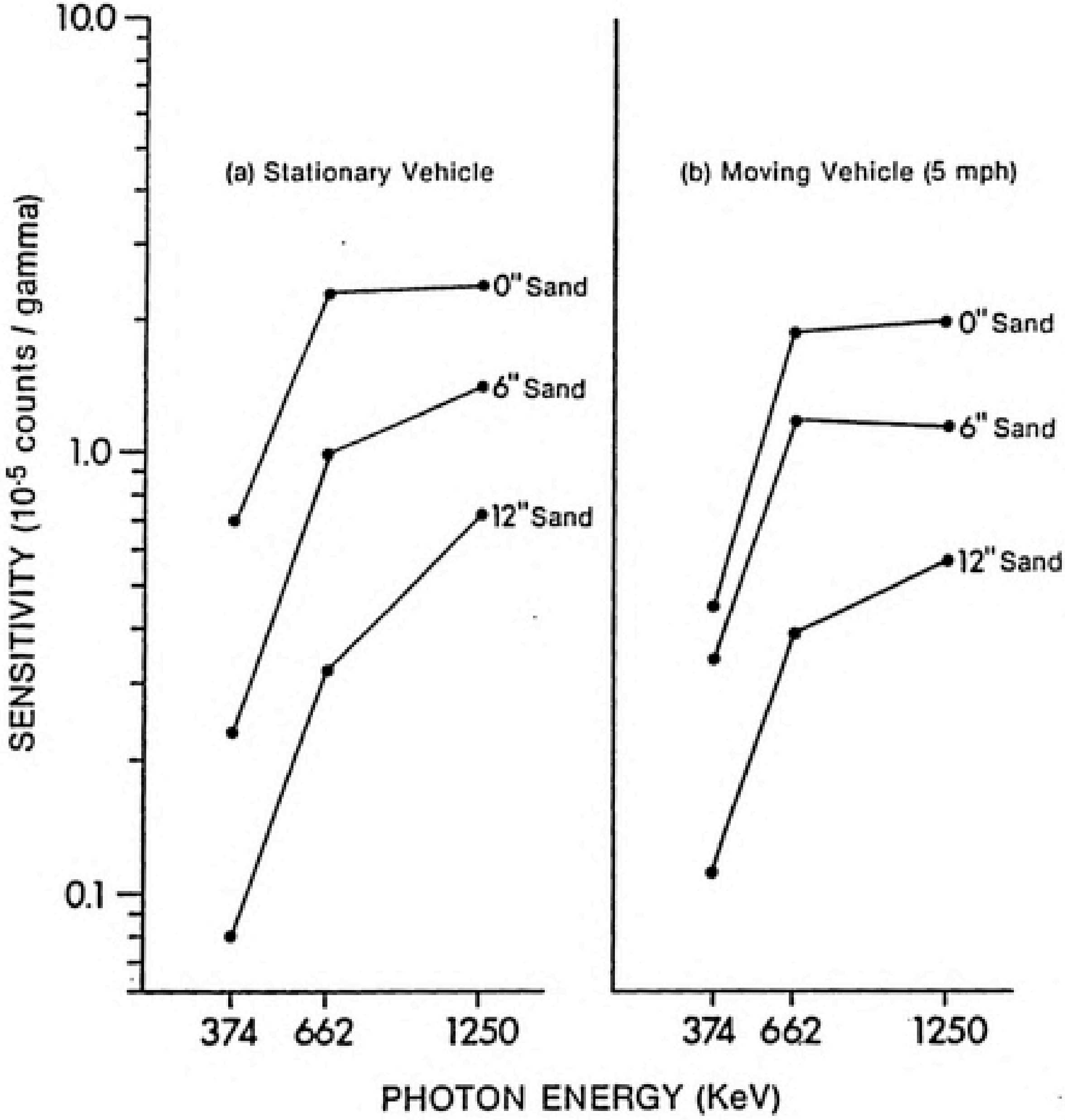

Figure 12. Sensitivity Curves for Stationary and Moving Vehicle, Brookhaven Sources

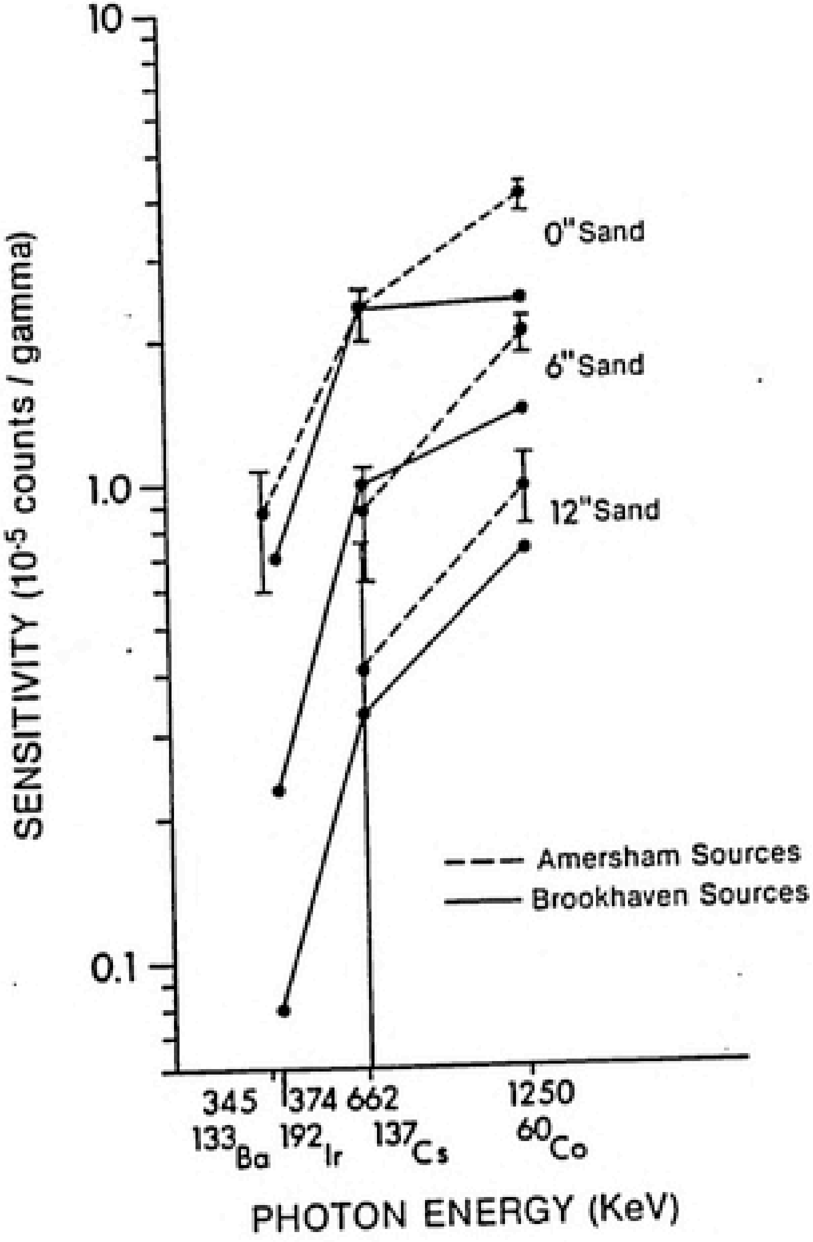

Figure 13. Comparison of Stationary-Vehicle Sensitivity Amersham and Brookhaven Sources

their higher activities. Standard deviations for these values were negligible and are not indicated on the curves. Appreciable uncertainties for the Amersham sources, given by the standard deviations of sensitivity, are shown on the curves representing these nuclides. Low activities of these sources contributed to the extent of the uncertainties. The error bars show the increase in uncertainty with the level of sand attenuation and decreasing energy.

Sensitivity for ^{133}Ba (345 KeV) is compared with that for ^{192}Ir (374 KeV) and is only indicated on the 0 inch sand level curve because of statistically insignificant values for ^{133}Ba at higher attenuation levels. With no sand attenuation in the truck, sensitivity values for the low energy nuclides of ^{133}Ba and ^{192}Ir were similar. The values were within a 20% difference.

Sensitivities for 662 KeV, obtained for the Amersham and Brookhaven sources of ^{137}Cs, were similar at all three sand attenuation levels. Differences between these values were within 22%.

At the 1250 KeV energy level, sensitivity for the Brookhaven ^{60}Co source was lower than that for the Amersham ^{60}Co source by as much as 41%. A possible explanation for this finding is the effect of dead time presented by the single channel analyzer (Amp/TSCA) which was incorporated into the system. Since dead time losses increase for greater emission rates, the greater activity of the Brookhaven ^{60}Co source would account for some drop in sensitivity.

The VPM electronics had been modified by BNL personnel during the time between the collection of data for the two sets of nuclides. Initially, the system incorporated an Amp/Preamp with which the Amersham sources were counted. Dead time determined for the original system, by the method described in Chapter III, was 3.5 μsec. The count rates obtained for the μCi sources were too small to be affected by dead time.

The Brookhaven sources were counted after the Amp/Preamp had been replaced by the Amp/TSCA. This change in the system increased the dead time from 3.5 μsec. to 16 μsec. The increase in the system's dead time and the greater emission rate of the mCi ^{60}Co source contributed to the drop in sensitivity values determined for the Brookhaven ^{60}Co source.

Dead time corrected sensitivity curves for the Brookhaven sources are presented in Figure 14 in comparison with the original curves for the Amersham sources. The corrected curves show a rise in sensitivity results for the Brookhaven ^{60}Co source but a discrepancy of up to 26% remains at the 1250 KeV energy level.

Dead time correction of the count rate observed for ^{192}Ir at 0" inches of sand increased the sensitivity for 374 KeV to a value which was 46% above that for the ^{133}Ba source (345 KeV). Correction of the high emission rate of

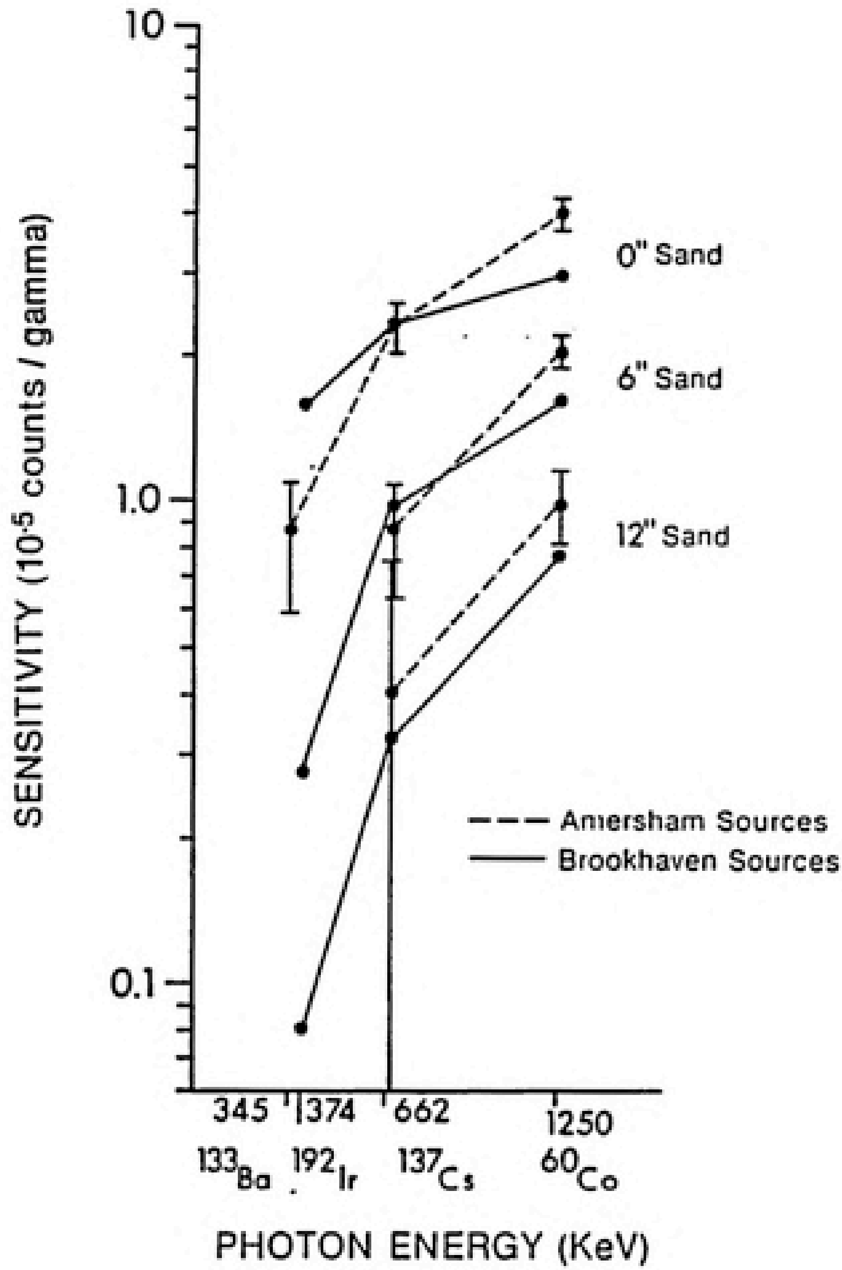

Figure 14. Comparison of Stationary-Vehicle Sensitivity, Amersham and Brookhaven Sources (Dead Time Corrected Values)

66 mCi of ^{192}Ir accounted for the increased sensitivity value at this point. Six inches of sand attenuated the intensity of the 374 KeV photons so that the count rate was affected by dead time correction to a lesser degree. Twelve inches of sand attenuated the intensity sufficiently so that the count rate, and hence sensitivity, remained unaffected by dead time correction.

At the 662 KeV energy level, correction of count rates for the 0.6 mCi ^{137}Cs source showed little or no effect on sensitivities for all attenuation levels. The interaction rate of this source was not high enough to be affected by dead time to any great degree. Sensitivity values for the Amersham and Brookhaven sources of ^{137}Cs remain in agreement, within 22%, for all attenuation levels.

Overall, the stationary-vehicle sensitivity values of the Amersham and Brookhaven sources show sufficient similarity to make meaningful comparison possible despite the fact that the system had been modified between data collections on the two sets of sources. Agreement is within 46% for the low energy sources of ^{133}Ba and ^{192}Ir, 22% for 662 KeV and 26% for 1250 KeV.

In summary, the sensitivity of the VPM in detecting the various sources counted in a stationary truck was dependent on

1. energy of photons emitted
2. sand attenuation level
3. dead time of the system.

The level of significance in sensitivity results was dependent on the activity of the source.

Comparison of moving-vehicle sensitivity with stationary-vehicle sensitivity is given in Figure 15. The curves represent dead time corrected sensitivity values for the Brookhaven sources counted on both a stationary and moving truck.

It was thought that the system would exhibit poorer sensitivity for sources counted on a moving vehicle than on a stationary vehicle because of changing source-to-detector geometry encountered with each pass over the detector. Results show moving-vehicle sensitivities were lower than stationary-vehicle values for all energies only at the 0 inch sand attenuation level.

The higher moving-vehicle sensitivities for ^{192}Ir and ^{137}Cs at 6 and 12 inches of sand attenuation realizes the possible effect of non-uniform attenuation presented by shielding materials moving over the detector. Stationary-vehicle sensitivities reflected the maximum shielding of the sand and the truck because of source alignment over the rear axle of the truck. Sources moving over the detector encountered maximum shielding only for a fraction of the counting interval. This was true because the differential in the rear axle of the truck was suspected to present a great deal of attenuation. When the axle moved over the detector, photons emitted isotropically from a source in the bed of the truck did not pass through

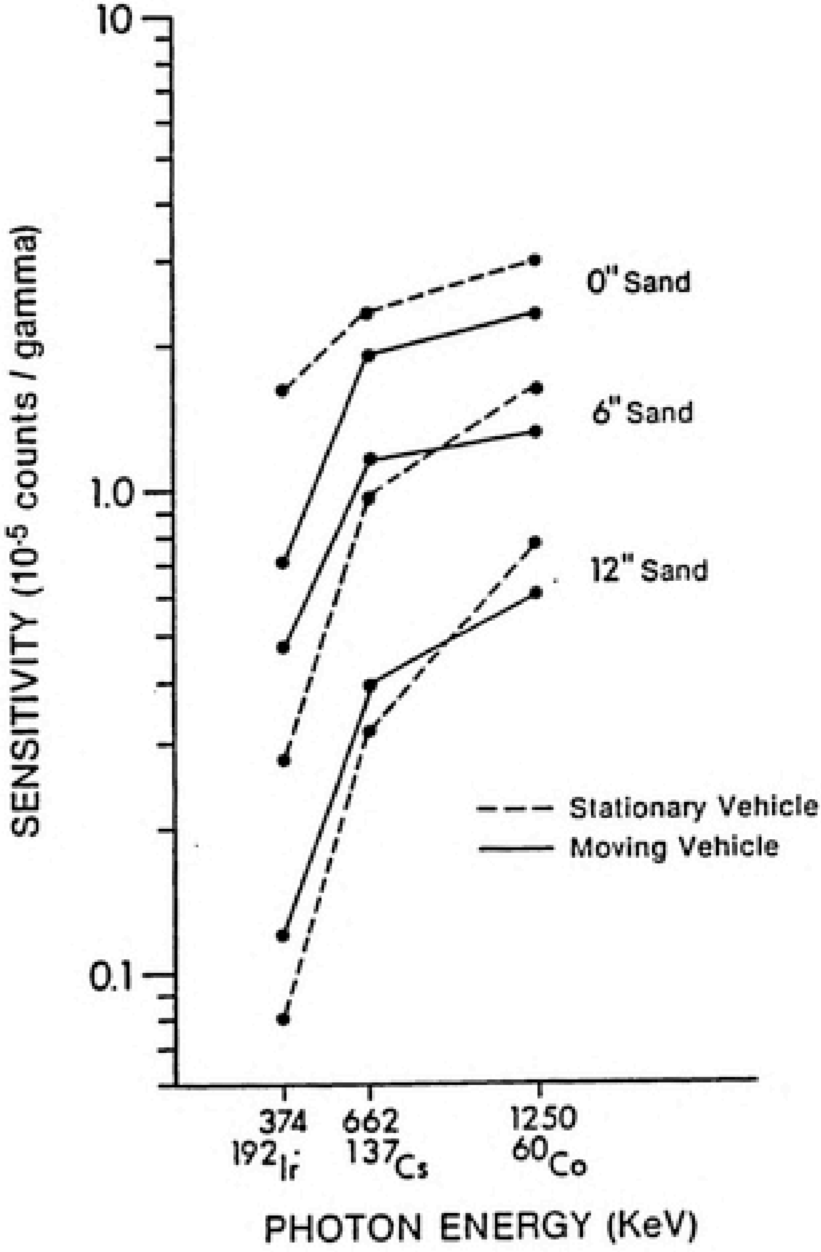

Figure 15. Comparison of Sensitivity for Brookhaven Sources (Dead Time Corrected Values) on Stationary and Moving Vehicle

the differential at all points of the pass during the counting interval. Therefore, for a greater fraction of the counting time, photons were attenuated only by the box of sand and the sheet metal of the truck bed.

Counting sources in a moving truck by making a series of runs over the detector presented a number of other variables. For example, paths taken over the detector varied somewhat between runs. Also the speed of each pass varied slightly. These variables could not be controlled absolutely, nonetheless, they did represent the practical situation for monitoring vehicles.

Possible explanations for discrepancies between stationary and moving vehicle sensitivities are listed below.

1. Changing source-to-detector geometry for moving truck
2. Non-uniform attenuation on moving truck
3. Variations in path over detector between runs
4. Variation in speed between runs
5. Dead time of the system.

Comparison of stationary and moving-vehicle sensitivities, show fairly good agreement between the two sets of values. The percents of difference between stationary and moving-vehicle sensitivity values for the

Brookhaven sources counted at three attenuation levels are given below.

Nuclide	0" Sand	6" Sand	12" Sand
^{192}Ir	56	40	33
^{137}Cs	17	17	18
^{60}Co	20	21	22

Lower Limits of Detection Curves

The LLD was determined from the net count rate observed for each of the nuclides counted in the truck at various levels of attenuation. Consequently, this parameter was subject to the influences of photon energy emitted, attenuation and dead time of the system. It was also dependent on background radiation and the activity of the source counted.

Given in units of activity (μCi), LLD was determined by the expression:

$$\frac{2.71 + 4.65\ (s_b)}{\text{net count rate}/\mu\text{Ci}} \quad .$$

Since net count rates increased with photon energy, the LLD was inversely proportional to the energy emitted. For example, the minimum detectable activity for a high energy nuclide was lower than that for a low energy nuclide. As net count rates decreased with additional attenuation, the minimum detectable activity increased, therefore, the LLD was proportional to attenuation. LLD results demonstrated the minimum detectable activity for a particular source counted at 12 inches of sand was higher than that for the same source counted at 6 inches of sand.

LLD values, given in μCi, were plotted versus sand attenuation level for each nuclide counted on the stationary and moving vehicle. It should be restated that the LLD serves as a guide for approximation of minimum detectable activity and does not denote an absolute level of activity that can or cannot be detected.

Figure 16 shows the LLD curves generated for each of the Amersham sources counted on a stationary truck. The curve for ^{133}Ba is limited to 0 and 3 inches of sand attenuation because of the lack of statistically significant net count rates observed for this source at 6 or more inches of sand attenuation on the truck. The curves show the upward trend of LLD for each nuclide with increasing attenuation and the reduction of minimum detectable activity with increasing photon energy emitted.

LLD values versus attenuation for the Brookhaven sources counted on the stationary and moving vehicle are presented graphically in Figure 17. All minimum detectable activities were determined from the dead time corrected net count rates for ^{192}Ir, ^{137}Cs and ^{60}Co.

Figure 17 (a) shows the LLD curves for the Brookhaven sources counted on a stationary truck. The curves show the upward trend of LLD with sand attenuation and reduction in LLD with energy emitted. However, there is

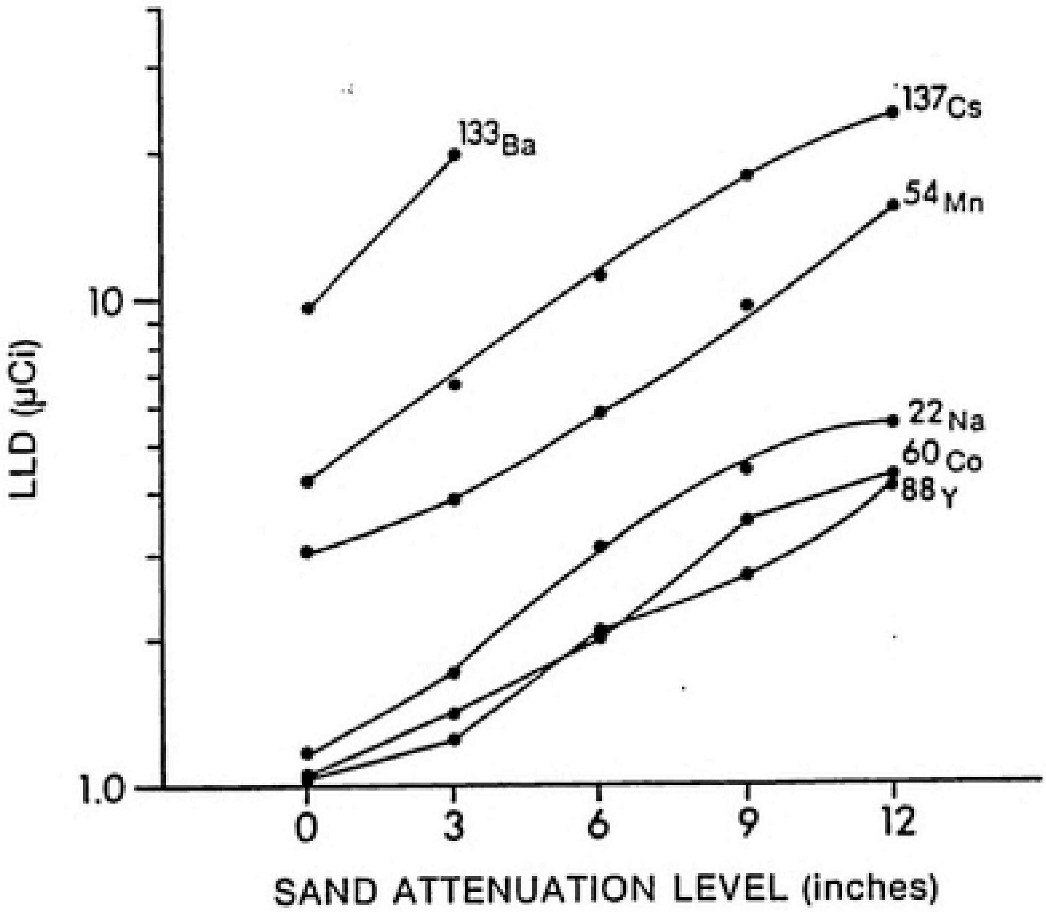

Figure 16. LLD Curves for Amersham Sources on Stationary Vehicle

is an irregularity at the 0 inch sand level. The curve for ^{192}Ir (374 KeV) shows a minimum detectable activity of 1.81 μCi at 0 inches of sand in contrast to the LLD value of 3.12 μCi for ^{137}Cs (662 KeV) at like attenuation. This finding is contrary to the statement that LLD is inversely proportional to photon energy.

A possible explanation for this result lies in the observation that 66 mCi of ^{192}Ir yielded a very high net count rate when counted in the empty truck. A possible error in the 16 μsec dead time factor would affect the LLD value for ^{192}Ir at 0 inches of sand to a greater degree than it would for ^{137}Cs at this point. The count rate for 0.6 mCi of ^{137}Cs was lower than that for 66 mCi of ^{192}Ir and , therefore, any error in dead time correction did not have as great an effect on the LLD value for ^{137}Cs.

For the purpose of comparison, LLD results for the Amersham sources are given by dashed curves in Figure 17 (a). The limited LLD curve for ^{133}Ba is shown for 0 and 3 inches of sand. LLD values for the low energy nuclides of ^{133}Ba and ^{192}Ir compared at 0 inches of attenuation showed a difference of 81%. A possible explanation for the disparity was the high net count rate elicited from 66 mCi of ^{192}Ir as opposed to the low rate observed for 8.96 μCi of ^{133}Ba.

Comparison of LLD curves for the 10.36 μCi and 0.6 mCi ^{137}Cs sources showed fairly good agreement, within 34%,

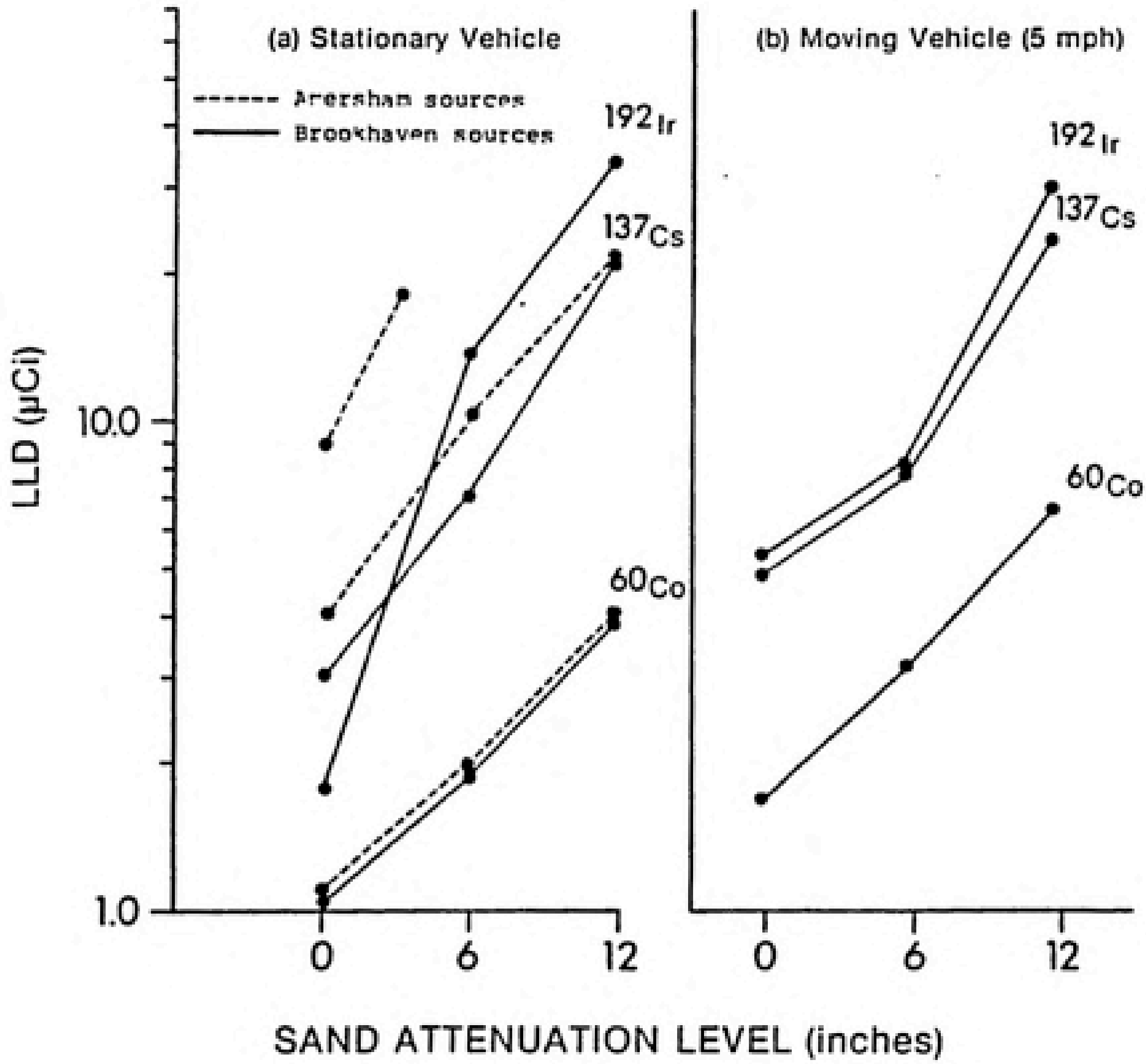

Figure 17. LLD Curves for Brookhaven Sources (Dead Time Corrected Values) on Stationary and Moving Vehicle

for the three attenuation levels represented. Agreement between LLD curves for the 10.12 μCi and 7.5 mCi ^{60}Co sources was within 5% for all sand attenuation levels.

Figure 17 (b) shows dead time corrected LLD curves for the Brookhaven sources counted on a moving vehicle. These results represented the practical situation for monitoring refuse trucks. The estimated minimum detectable activity for ^{192}Ir on a truck moving at 5 mph over the detector ranged from 5.51 to 31.42 μCi for three sand attenuation levels. For ^{137}Cs the minimum detectable activity ranged from 5.00 to 24.68 μCi. The high energy ^{60}Co source demonstrated a range of minimum detectable activity from 1.73 to 6.78 μCi over all attenuation levels.

Chapter VI

CONCLUSION AND RECOMMENDATIONS

The use of NaI for detection of gamma emitting radionuclides has been well established. The excellent detection efficiency of this medium made the VPM well suited for monitoring purposes. Results of sensitivity testing on a stationary truck demonstrated good performance by the VPM in the detection of μCi amounts of radionuclides ranging in energy from 345 to 1836 KeV.

A limit of the system's sensitivity was observed at the 345 KeV energy level for the 8.96 μCi source of ^{133}Ba counted at 6 or more inches of sand attenuation in the truck. Detection sensitivity for the low energy source of ^{192}Ir (374 KeV), counted at 6 and 12 inches of sand attenuation, was demonstrated because of the greater activity (66 mCi) of this source.

Sources counted in the moving truck ranged in energy from 374 to 1250 KeV. Moving-vehicle sensitivity results demonstrated that mCi amounts of ^{192}Ir, ^{137}Cs and ^{60}Co were easily detected at all attenuation levels represented.

The monitoring modality of the VPM proved to be an effective method for documenting radioactivity on a truck passing over the detector. Radiation levels were recorded by a print-out of count rates measured by the counter/timer as well as registered by the strip chart recorder.

LLD results provided estimates of minimum detectable activities for the nuclides used in testing and also gave an indication of the amount of a radionuclide that can escape detection. Under testing conditions of 0 to 12 inches of sand attenuation in the stationary pickup truck, the ranges of minimum detectable activities for the Amersham sources are given below.

Nuclide	Activity at Testing (μCi)	Range of LLD (μCi)
^{133}Ba	8.96	9.60 - 19.90*
^{137}Cs	10.36	4.21 - 23.58
^{54}Mn	8.76	3.03 - 15.34
^{22}Na	10.30	1.16 - 5.45
^{60}Co	10.12	1.03 - 4.13
^{88}Y	5.08	1.02 - 4.28

* LLD values for ^{133}Ba were not determined for attenuation levels of 6 or more inches of sand.

Ranges of minimum detectable activities for the Brookhaven sources counted at 0 to 12 inches of sand attenuation on the pickup truck moving at 5 mph over the detector are given below. These values of LLD were determined from dead time corrected counting data.

Nuclide	Activity at Testing (mCi)	Range of LLD (μCi)
^{192}Ir	66.0	5.51 - 31.42
^{137}Cs	0.6	5.00 - 24.68
^{60}Co	7.5	1.73 - 6.78

From results of sensitivity testing and LLD determination it can be concluded that the VPM may be used to monitor vehicles for μCi amounts of radionuclides which emit photon energies above 345 KeV. It should be noted that the sensitivity of the VPM is strictly limited to gamma emitting radionuclides. Since alpha or beta emissions will not penetrate surrounding materials to interact with the NaI crystal, the system would be blind to large amounts of pure alpha or beta emitters.

Results presented in this report pertain to testing the system with a standard-sized pickup truck. Although any sized vehicle may transport refuse to the landfill, large garbage trucks are routinely used for this purpose. Larger trucks may present greater source-to-detector distances and possibly increased shielding. These variables may affect the performance of the VPM. As a recommendation, it would be useful to investigate the system's sensitivity for a source placed above a full load on a garbage truck.

Another recommendation is to relocate the VPM to the gate of the landfill since the present site does not cover every access. This action would ensure surveillance and make cooperation of the drivers more easily achievable.

A speed bump placed in front of the pressure tube would ensure a proper speed at which to monitor the contents of a truck. If necessary, an audible alarm may be incorporated into the system to alert truck drivers to the presence of radioactive contamination.

The present test site was allocated to test the system and to determine the proportion of contaminated landfill traffic. Relocation of the VPM will be contingent on the extent of the problem of contaminated refuse and on cost justification to be determined by SEPD personnel.

The objectives of this project have been satisfied with the development of the VPM system and its placement at the test site. Performance of the system has been documented and shows that it is suited to the purpose of monitoring μCi amounts of radioactive contamination on landfill refuse traffic.

APPENDIX I

Method for Determining Sensitivity

To calculate sensitivity for various photon energies of the Amersham sources, the photon emission rate of each energy must first be determined. Expressed in gammas per minute (gpm), the photon emission rate was determined from the activity of the source in μCi, a conversion factor for disintegrations per minute (dpm) per μCi and the photon emission probability in gammas per disintegration (g/d) (Table 1). This method is given by

$$(\mu Ci)\quad (2.22 \times 10^{6}\ dpm/\mu Ci)\quad (g/d) = gpm$$

Sensitivity was then determined from the net count rate (Table 7) divided by the photon emission rate gpm. Sensitivity, expressed in the number of counts per gamma (c/g) is given by

$$\text{Sensitivity} = \frac{\text{net count rate (cpm)}}{\text{photon emission rate (gpm)}} = c/g$$

For nuclides emitting photons of one discrete energy the determination of sensitivity was straight forward.

Consider, for example, the 10.36 μCi source of ^{137}Cs which emits photons of 662 KeV with a photon emission probability of 0.85 g/d. The photon emission rate for ^{137}Cs was determined by

$$(10.36\ \mu Ci)\ (2.22 \times 10^{6}\ dpm/\mu Ci)\ (0.85\ g/d) = 1.95 \times 10^{7}\ gpm.$$

Sensitivity for 662 KeV at 0 inches of sand attenuation in the truck was determined as follows: Net count rates (cpm) for the Amersham sources are listed in Table 7.

$$\text{Sensitivity} = \frac{448\ \text{cpm}}{1.95 \times 10^{7}\ \text{gpm}} = 2.30 \times 10^{-5}\ \text{c/g}$$

Similarly, the sensitivity for 662 KeV

at 3" sand = 1.46×10^{-5} c/g

at 6" sand = 0.87×10^{-5}

at 9" sand = 0.54×10^{-5}

at 12" sand = 0.41×10^{-5}

The same procedure was used to determine the sensitivity for the 8.76 μCi source of ^{54}Mn which emits photons of 834 KeV at a photon probability of 1.00 g/d.

Sensitivity for 834 KeV

at 0" sand = 2.71×10^{-5} c/g

at 3" sand = 2.15×10^{-5}

at 6" sand = 1.41×10^{-5}

at 9" sand = 0.86×10^{-5}

at 12" sand = 0.54×10^{-5}

For nuclides emitting two or more photon energies that do not vary widely, a single energy was determined by a weighted average of the multiple energies. Sensitivities, in this case, were determined for the average photon energy emitted.

Consider the 10.12 μCi source of ^{60}Co which emits photons of 1173 and 1332 KeV. The weighted average of 1250 KeV was used to represent the energy emitted by ^{60}Co. The weighted average of approximately 1250 KeV [(1173 + 1332)/2] was used to represent the energy emitted by ^{60}Co. (The error introduced into estimation of sensitivity by use of this weighted average is less than 2%.) The photon emission rate was determined by the same procedure using a photon probability of 2.00 g/d.

Sensitivity for 1250 KeV

at 0" sand $= 3.98 \times 10^{-5}$ c/g

at 3" sand $= 2.96 \times 10^{-5}$

at 6" sand $= 2.08 \times 10^{-5}$

at 9" sand $= 1.18 \times 10^{-5}$

at 12" sand $= 0.99 \times 10^{-5}$

For the 8.96 μCi source of ^{133}Ba, a photon energy of 345 KeV represented a weighted average of several similar energies emitted. The various energies of ^{133}Ba and their percent yield were 276 KeV (7%), 302 KeV (14%), 356 KeV (69%), and 382 KeV (8%). The total photon probability was

0.98 g/d from which the photon emission rate was determined.

Sensitivity for 345 KeV

$$\text{at } 0'' \text{ sand} = 0.87 \times 10^{-5} \text{ c/g}$$
$$\text{at } 3'' \text{ sand} = 0.42 \times 10^{-5}$$

Sensitivity for 345 KeV at 6 or more inches of sand attenuation was not determined.

To determine sensitivities for two widely varying photon energies emitted by one nuclide, a somewhat different procedure was used. First, it was necessary to determine the emission rate for each energy emitted. Then, the estimated count rate for each energy was determined.

For example, in the case of the 10.30 μCi source of ^{22}Na, the energies emitted are 1274 KeV and 511 KeV with photon probabilities of 1.00 and 1.80 g/d respectively. Using the previously described procedure, the respective emission rates were determined to be 2.29×10^7 gpm and 4.12×10^7 gpm.

Since the 1274 KeV photon energy of ^{22}Na was similar to the 1250 KeV photon energy of ^{60}Co, it was assumed that the sensitivity determined for 1250 KeV could be used to represent the 1274 KeV energy.

Hence, the sensitivity for 1274 Kev

$$\text{at } 0'' \text{ sand} = 3.98 \times 10^{-5} \text{ c/g}$$
$$\text{at } 3'' \text{ sand} = 2.96 \times 10^{-5}$$

at 6" sand $= 2.08 \times 10^{-5}$

at 9" sand $= 1.18 \times 10^{-5}$

at 12" sand $= 0.99 \times 10^{-5}$

To estimate the count rate for the 1274 KeV photons, the photon emission rate was multiplied by the 1274 KeV sensitivity. At 0 inches of sand, for example, the estimated count rate is given by

$$(2.29 \times 10^{7} \text{ gpm})\ (3.98 \times 10^{-5} \text{ c/g}) = 911 \text{ cpm.}$$

By subtracting this count rate from the total net count rate observed for ^{22}Na (Table 7), the estimated count rate for the 511 KeV photons was determined. The 511 KeV count rate was then divided by the photon emission rate for 511 KeV to yield the sensitivity for this energy.

For example, sensitivity for 511 KeV at 0 inches sand was determined by

$$\frac{1624 - 911 \text{ cpm}}{4.12 \times 10^{7} \text{ gpm}} = 1.73 \times 10^{-5} \text{ c/g}$$

Similarly

at 3" sand $= 0.98 \times 10^{-5}$ c/g

at 6" sand $= 0.32 \times 10^{-5}$

at 9" sand $= 0.38 \times 10^{-5}$

at 12" sand $= 0.28 \times 10^{-5}$

A similar procedure was used to determine sensitivities for the 898 KeV and 1836 KeV photon energies emitted by the 5.08 μCi source of ^{88}Y. The respective photon emission probabilities of 0.934 and 0.993 g/d were used to determine the photon emission rates for each energy as was done previously. The emission rate for each energy is given as

$$898 \text{ KeV} = 1.06 \times 10^{7} \text{ gpm}$$
$$1836 \text{ KeV} = 1.12 \times 10^{7} \text{ gpm}$$

Since the 898 KeV photon energy was similar to the 834 KeV energy emitted by ^{54}Mn, it was assumed that the sensitivities determined for 834 KeV could be used to represent the 898 KeV energy of ^{88}Y.

Hence the sensitivity for 898 KeV

$$\text{at } 0'' \text{ sand} = 2.71 \times 10^{-5} \text{ c/g}$$
$$\text{at } 3'' \text{ sand} = 2.15 \times 10^{-5}$$
$$\text{at } 6'' \text{ sand} = 1.41 \times 10^{-5}$$
$$\text{at } 9'' \text{ sand} = 0.86 \times 10^{-5}$$
$$\text{at } 12'' \text{ sand} = 0.54 \times 10^{-5}$$

Sensitivity for 1836 KeV was determined from the estimated count rate for 1836 KeV photons by a procedure similar to that previously described for 5111 KeV.

Sensitivity for 1836 KeV

at 0" sand = 5.57×10^{-5} c/g

at 3" sand = 4.69×10^{-5}

at 6" sand = 2.77×10^{-5}

at 9" sand = 2.29×10^{-5}

at 12" sand = 1.42×10^{-5}

Propagation of Error

To determine the standard deviation of net count rates in counts per minute (cpm) the following procedure was used:

$$s_{net\ cpm} = 2\sqrt{\frac{s_g^2 + s_b^2}{DF_L}}$$

where

s_g = standard deviation of gross counts/30 seconds (Table 5)

s_b = standard deviation of background counts/30 seconds (Table 5)

DF_L = distance factor to correct count rate to 12" above bed of truck from sand level L.

For example, consider the determination of standard deviation of net count rate (cpm) for the 662 KeV photons emitted by ^{137}Cs counted in the truck at 0 inches of sand attenuation.

$$s_{net\ cpm} = 2\sqrt{\frac{30^2 + 19^2}{1.96}} = 50 \text{ cpm.}$$

The standard deviation of sensitivity values for the single energies emitted by ^{133}Ba, ^{137}Cs, ^{54}Mn and ^{60}Co was determined using the following method:

$$s_{\text{Sensitivity}} = \frac{s_{\text{net cpm (E) (L)}}}{\text{photon emission rate (gpm) for energy (E)}}$$

where

$s_{\text{net cpm}}$ = standard deviation of net count rate (cpm) for source of energy (E) counted at sand attenuation level (L) (Table 7).

For example, the photon emission rate for the 662 KeV photons emitted by ^{137}Cs was 1.95×10^7 gpm. The standard deviation of the sensitivity for 662 KeV photons at 0 inches of sand in the truck was determined by

$$s_{\text{sensitivity}} = \frac{50 \text{ cpm}}{1.95 \times 10^7 \text{ gpm}} = 0.26 \times 10^{-5} \text{ c/g.}$$

The standard deviation of sensitivity values for the two distinct photon energies emitted by ^{22}Na and ^{88}Y was determined by a different procedure.

Consider the distinct energies, emitted by ^{22}Na of 1274 KeV and 511 KeV. Since the 1274 KeV photon energy was similar to the 1250 KeV photon energy of ^{60}Co, the standard deviation of sensitivity for 1250 KeV was used for the standard deviation of sensitivity for 1274 KeV photons. Therefore, the standard deviation of sensitivity for the 1274 KeV photons at 0 inches sand $= 0.22 \times 10^{-5}$ c/g

at 3 inches sand $= 0.13 \times 10^{-5}$

at 6 inches sand $= 0.12 \times 10^{-5}$

at 9 inches sand $= 0.10 \times 10^{-5}$

at 12 inches sand $= 0.15 \times 10^{-5}$

The next step was to determine the standard deviation of the estimated net count rate for the 1274 KeV photons. This was done by multiplying the standard deviation of sensitivity for 1274 KeV photons by the photon emission rate for 1274 KeV photons. For example, the standard deviation of the estimated count rate for 1274 KeV photons at 0 inches of sand is given by

$$s_{1274\text{ KeV cpm}} = 0.22 \times 10^{-5}\text{ c/g } (2.29 \times 10^{7}\text{ gpm})$$
$$= 50\text{ cpm}$$

The standard deviation of sensitivity for the 511 KeV photon energy emitted by ^{22}Na was determined by:

$$s_{511\text{ KeV sensitivity}} = \frac{\sqrt{s^2_{\text{net cpm, Na}} + s^2_{1274\text{ Kev cpm}}}}{511\text{ KeV photon emission rate}}.$$

where

$s_{\text{net cpm, Na}}$ = standard deviation of the total net cpm of ^{22}Na (Table 7)

$s_{1274\text{ KeV cpm}}$ = standard deviation of estimated count rate for 1274 KeV photons

511 KeV photon emission rate $= 4.12 \times 10^{7}$ gpm

For example, the standard deviation of sensitivity for 511 KeV photons at 0 inches of sand is given by

$$s_{511\text{ KeV sensitivity}} = \frac{\sqrt{98^2 + 50^2}\text{ cpm}}{4.12 \times 10^7\text{ gpm}} = 0.27 \times 10^{-5}\text{ c/g}$$

APPENDIX II

<u>Method for Determining Dead Time Corrected Sensitivity</u>

To calculate the sensitivity of the system for the Brookhaven sources with the increased dead time of 16 µsec. presented by the Amp/TSCA, the photon emission rate (gps) was determined by

$$(\mathrm{mCi})\ (3.70 \times 10^7\ \mathrm{dps/mCi})\ (\mathrm{g/d}) = \mathrm{gps.}$$

The dead time corrected net count rate was determined by

$$\frac{n}{(1 - nT)} - \text{background rate} = \text{cps}$$

where

n = observed rate (cps)

T = 16 µsec. dead time

Dead time corrected sensitivity was determined by the quotient of dead time corrected net rate and the photon emission rate, i.e.

$$\text{Dead time corrected sensitivity} = \frac{\text{corrected net rate (cps)}}{\text{photon emission rate (gps)}}$$

Consider, for example, the 66 mCi source of ^{192}Ir which emits an average photon energy of 374 KeV, with a photon emission probability of 2.08 gammas per disintegration (g/d). The photon emission rate (gps) was determined by

$$(66 \text{ mCi})\ (3.70 \times 10^{7} \text{ dps/mCi})\ (2.08 \text{ g/d}) = 5.08 \times 10^{9} \text{ gps}$$

From Table 9, the observed gross rate for ^{192}Ir at 0 inches of sand attenuation was 1066641 counts/30 seconds and was converted to 35555 counts/second. The background rate was 7 counts/second. The dead time corrected net count rate is given by

$$\frac{35555 \text{ cps}}{1 - 35555\ \ (16 \times 10^{-6} \text{ sec})} - 7 \text{ cps} = 82464 \text{ cps}$$

Similarly, the dead time corrected sensitivity for 347 KeV

at 6 inches sand $= 0.28 \times 10^{-5}$ c/g

at 12 inches sand $= 0.08 \times 10^{-5}$ c/g.

All sensitivities for the Brookhaven sources were corrected for dead time by the same method.

APPENDIX III

<u>Method for Determining Lower Limits of Detection</u>

LLD's were determined for sources counted on a stationary vehicle at various sand attenuation levels by the following method:

$$LLD = \frac{2.71 + 4.65\ (s_b)}{\bar{x}}$$

where

s_b = standard deviation of background counts/30 seconds

$$\bar{x} = \frac{\text{average net counts/30 seconds}}{\mu\text{Ci}}$$

To determine the standard deviation of LLD the following expression was used:

$$s_{LLD} = \frac{A\ (s_{\bar{x}})}{\bar{x}^2}$$

where

$A = 2.71 + 4.65\ (s_b)$

$$\bar{x} = \frac{\text{average net counts/30 seconds}}{\mu\text{Ci}}$$

s_x = standard deviation of x

For example, consider the 10.36 μCi source of ^{137}Cs counted at 0" of sand attenuation in the stationary truck. The net counts/30 sec are listed in Table 6.

$$\text{LLD} = \frac{2.71 + 4.65\ (19\ \text{counts/30 seconds})}{\dfrac{224\ \text{counts/30 seconds}}{10.36\ \mu\text{Ci}}} = 4.21\ \mu\text{Ci}$$

$$s_{\text{LLD}} = \frac{2.71 + 4.65\ (19\ \text{counts/30 sec})\left[\dfrac{25\ \text{counts/30 sec}}{10.36\ \mu\text{Ci}}\right]}{\left[\dfrac{224\ \text{counts/30 sec}}{10.36\ \mu\text{Ci}}\right]^2}$$

$$= 0.47\ \mu\text{Ci}$$

The LLD's for all the Amersham sources were determined using this same procedure.

LLD values for the Brookhaven sources were determined from dead time corrected count rates by the following procedures. For the Brookhaven sources counted on a stationary vehicle, the gross counts/30 seconds (Table 9) were converted to gross counts per second (cps). The gross cps were corrected for dead time by

$$N = \frac{n}{1 - nT}$$

where

N = dead time corrected gross rate (cps)

n = observed gross count rate (cps)

T = dead time of 16 μsec.

The background rate (cps) was subtracted from the dead time corrected gross rate to determine the dead time corrected net rate (cps).

The dead time corrected net rate (cps) was converted back to counts/30 seconds and used in the expression for determining LLD. LLD values for the Brookhaven sources counted on a stationary vehicle were determined by

$$\text{LLD} = \frac{2.71 + 4.65\ (s_b)}{\text{dead time corrected net counts/30 sec/}\mu\text{Ci}} = \mu\text{Ci}$$

For example, consider the 0.6 mCi source of ^{137}Cs counted at 0 inches of sand in the stationary truck. From Table 9, the gross rate was 13145 counts/30 seconds and the background rate was 209 counts/30 seconds. Dividing these rates by 30, the gross rate for the ^{137}Cs source and background were 438 cps and 7 cps respectively.

The dead time corrected net rate (cps) for ^{137}Cs was determined by

$$\frac{438\ \text{cps}}{1 - 438\ \text{cps}\ (16 \times 10^{-6}\ \text{sec})} - 7\ \text{cps} = 434\ \text{cps.}$$

Multiplying by 30 converted the dead time corrected net rate of 434 cps to 13020 counts/30 seconds. The LLD for ^{137}Cs counted at 0 inches of sand was determined by

$$LLD = \frac{2.71 + 4.65\ (14\ \text{counts}/30\ \text{sec})}{13020\ \text{counts}/30\ \text{sec}/600\ \mu\text{Ci}} = 3.12\ \mu\text{Ci}$$

LLD values were determined for all Brookhaven sources on a stationary vehicle by the above procedure.

A similar procedure was used for determining LLD for the Brookhaven sources counted on a moving vehicle. The moving-vehicle gross counts/4 seconds are given in Table 15.

For example, the observed rate for 7.5 mCi of ^{60}Co counted at 0 inches of sand was 43052 counts/4 seconds. The background rate was 34 counts/4 seconds. Dividing by 4 converted the gross rate for the ^{60}Co source and the background rate to 10763 cps and 9 cps respectively. The dead time corrected net rate (cps) for ^{60}Co was determined by

$$\frac{10763\ \text{cps}}{1 - 10763\ \text{cps}\ (16 \times 10^{-6}\ \text{sec})} - 9\ \text{cps} = 12993\ \text{cps}.$$

Multiplying by 4 converted the dead time corrected net rate (cps) to 51972 counts/4 seconds. Determination of LLD for ^{60}Co counted at 0 inches of sand is given by

$$LLD = \frac{2.71 + 4.65\ (2\ \text{counts}/4\ \text{sec})}{51972\ \text{counts}/4\ \text{sec}/7500\ \mu\text{Ci}} = 1.73\ \mu\text{Ci}$$

LLD values for all Brookhaven sources counted on a moving vehicle were determined by the above procedure.

BIBLIOGRAPHY

Balsamo, J. (BNL) Personal Communication 1984.

Bianco, J., Canberra Industries, Personal Communication 1985.

Cember, H., Introduction to Health Physics, 2nd ed., Pergamon Press, New York, 1983, p 114.

Colle, R., et al., "Upgrading Environmental Radiation Data", Health Physics Society Committee Report No. 1, Office of Radiation Programs U.S. Environmental Protection Agency, Washington, D.C., 1980, pp. 6-24 to 6-26.

Currie, L.A., "Limits for Qualitative Detection and Quantitative Determination", Anal. Chem., Vol. 40, No. 3, March, 1968, pp. 586-93.

Dvorak, R. (LANL) Personal Communication 1984.

Health Physics Society Newsletter, Vol. XII, No. 5, May 1984.

Knoll, G.F., "General Properties of Radiation Detectors", Radiation Detection and Measurement, Wiley, New York, 1979, p. 95.

National Council on Radiation Protection and Measurements, "A Handbook of Radioactivity Measurements Procedures", NCRP Report No. 58, 1978, p. 60.

Remington, R.D., Shork, M.A., "Hypothesis Testing", Statistics with Applications to the Biological and Health Sciences, Prentice-Hall, Englewood Cliffs, N.J., 1970, p. 192.